SERI/TR-253-3549
UC Category: 262
DE90000315

SERI/TR--253-3549

DE90 000315

Innovative Turbine Concepts for Open-Cycle OTEC

Final Report of Work Performed by
Massachusetts Institute of Technology
Texas A&M University
University of Pennsylvania

December 1989

SERI Contact: J. M. Parsons

Prepared under Task No. OE912032

Solar Energy Research Institute
A Division of Midwest Research Institute

1617 Cole Boulevard
Golden, Colorado 80401-3393

Prepared for the
U.S. Department of Energy
Contract No. DE-AC02-83CH10093

NOTICE

Printed in the United States of America
Available from:
National Technical Information Service
U.S. Department of Commerce
5285 Port Royal Road
Springfield, VA 22161

Price: Microfiche A01
Printed Copy A04

Codes are used for pricing all publications. The code is determined by the number of pages in the publication. Information pertaining to the pricing codes can be found in the current issue of the following publications which are generally available in most libraries: *Energy Research Abstracts (ERA)*; *Government Reports Announcements* and Index (*GRA* and I); *Scientific and Technical Abstract Reports (STAR)*; and publication NTIS-PR-360 available from NTIS at the above address.

PREFACE

This report summarizes the results of preliminary studies conducted to identify and evaluate three innovative concepts for an open-cycle ocean thermal energy conversion (OTEC) steam turbine that have the potential to significantly reduce the cost of OTEC electrical power plants. The three concepts are (1) a crossflow turbine, (2) a vertical-axis, axial-flow turbine, and (3) a double-flow, radial-inflow turbine with mixed-flow blading. In all cases, the innovation involves the use of lightweight, composite plastic blading and a physical geometry that facilitates efficient fluid flow to and from the other major system components and reduces the structural requirements for the turbine or the system vacuum enclosure, or both. The performance, mechanical design, and cost of each of the concepts are developed to varying degrees but in sufficient detail to show that the potential exists for cost reduction to the goals established in the U.S. Department of Energy's (DOE's) planning documents.

This work was completed under funding provided by DOE's Ocean Energy Technology Division. Work at the Solar Energy Research Institute was performed under contract no. DE-AC02-83CH10093 with the U.S. Department of Energy.

Approved for

SOLAR ENERGY RESEARCH INSTITUTE

R. G. Nix, Program Manager
Ocean Energy Technology Program

L.M. Murphy, Director
Solar Heat Research Division

SUMMARY

This is a summary report of three university studies that dealt with innovative steam turbine design and construction concepts aimed at significantly reducing the cost of turbines for use in an open-cycle ocean thermal energy conversion (OTEC) power and desalinated water production plant. Previous OTEC studies were directed at large plants in the 100-MW_e size range and required steam turbines outside the state of the art. Recent studies of plants in the 10-MW_e range identified turbines that could be constructed using existing industry components and technology for open-cycle OTEC plants with little technical risk. Preliminary cost projections on these plants indicate that significant cost reductions in the hardware are necessary to produce power or desalinated water, or both, competitively.

This study was completed in parallel with other activities in the federal Ocean Energy Technology Program directed to the design and construction of turbine hardware using existing industry technology and equipment. This hardware will be built and tested in a system experiment designed to show the technical feasibility of net power production in an open OTEC cycle. These earlier experimental results, in combination with the results of this study, will provide the data needed to confidently assess the economic feasibility of larger-scale open-cycle OTEC power plants.

Three turbomachinery concepts were identified and evaluated in this study. They reflect the three major types of turbine blading in use in the industry today: axial, radial, and mixed-flow configurations. The approach used was (1) to determine the key operating and design parameters of a turbine for this application by analysis of maximum obtainable performance, (2) to specify the mechanical design of the hardware associated with a 2-MW_e system, and (3) to generate an estimate of the cost to produce the design defined in the study. The results of the studies showed that all three blade types examined could be developed into viable options and that the final determination of the best approach would require more detailed definition of each turbine and its interface with other system components than was possible in preliminary evaluations.

The following additional conclusions have an important bearing on the final choice of the direction that should be taken in turbine development.

1. Maximum efficiency is not the overriding criterion for choosing the design and operating parameters for an open-cycle OTEC turbine (in contrast to conventional power plants) when the use of existing hardware is considered. These results showed, for example, that an axial turbine operating with a 33% higher steam throughput and a 7% lower efficiency than the most efficient configuration provides the most cost-effective open-cycle OTEC system.
2. The use of alternative materials for turbine blading, such as composite blading, can be justified on the basis of OTEC operating conditions. It should result in a lighter, less expensive turbine wheel and support structure than are currently possible.
3. The vacuum enclosure, a major system cost item, can be significantly modified to reduce its cost by establishing better or more suitable interfaces between the turbine and the rest of the system. Vertical

orientation of the axial-flow system and multiple flow arrangements of the other two options can achieve that. The size and cost of the turbine enclosure can thus be reduced and the performance of the turbine improved.

TABLE OF CONTENTS

TABLE OF CONTENTS (Concluded)

LIST OF FIGURES

LIST OF TABLES

1.0 INTRODUCTION

1.1 Background

The vast amount of heat stored in the surface layers of the Earth's oceans offers tremendous potential for conversion into useful mechanical and electrical energy, on a scale that could have a significant impact on the energy economies of nations with access to tropical or semitropical seawater. The energy that can be produced as a result of the difference in temperatures between this warm water and the cold water that exists at the oceans' depths has been the subject of much research on closed and open ocean thermal energy conversion (OTEC) cycles [1,2,3].

Several thermoeconomic analyses of the feasibility of producing electricity by using open-cycle conversion of the thermal resource in tropical and semitropical oceans have concluded that near-term penetration of certain small island markets may be possible with current technology. The longer-range development of the technology into more competitive markets, however, requires the development of new technical approaches to large, seawater piping systems and turboconversion equipment [4,5].

The open-cycle OTEC system, as currently conceived, is built of power system modules that consist of a turbine, an evaporator, a condenser, and an exhaust diffuser (if necessary). A concept for the assembly of these power modules onto a seawater pumping and distribution system is shown in Figure 1-1. The seawater systems and the vacuum purge system designs would be sized to meet the plant's total required output. Energy conversion would occur in multiple power modules. The number of power modules needed to meet the plant's output requirement is determined by the electrical capacity of each module. The capacity (or output) of each power module is determined by the size, number, and steam throughput of turbine rotors contained in each module.

Recent studies have suggested that low-pressure (LP) stages of a nuclear turbine could be adapted, through appropriate redesign of the stator row, to operate satisfactorily as an open-cycle OTEC turbine. Since such a turbine would be well characterized thermally, structurally, and dynamically, it could be considered an option for a prototype open-cycle power plant [4]. A rough estimate of the performance and cost of such a turbine indicates that a single-flow configuration could produce a power output of 1.4 MW_e at a total to static efficiency of 78% [6].

A single-flow axial configuration is estimated to cost $2 million (±20%). A percentage breakdown of turbine component costs is as follows:

Rotor blading	26%-30%
Casing	24%-30%
Disk and shaft	15%-20%
Bearing and lube system	6%-8%
Valves and piping	8%-10%
Others (controls, seals, pedestal, fixed blading, etc.)	21%

When the cost of the generator and switch gear is added to these numbers, the total cost of an open-cycle OTEC turbine/generator assembly that uses slightly modified existing hardware is estimated to be almost $2500/$kW_e$.

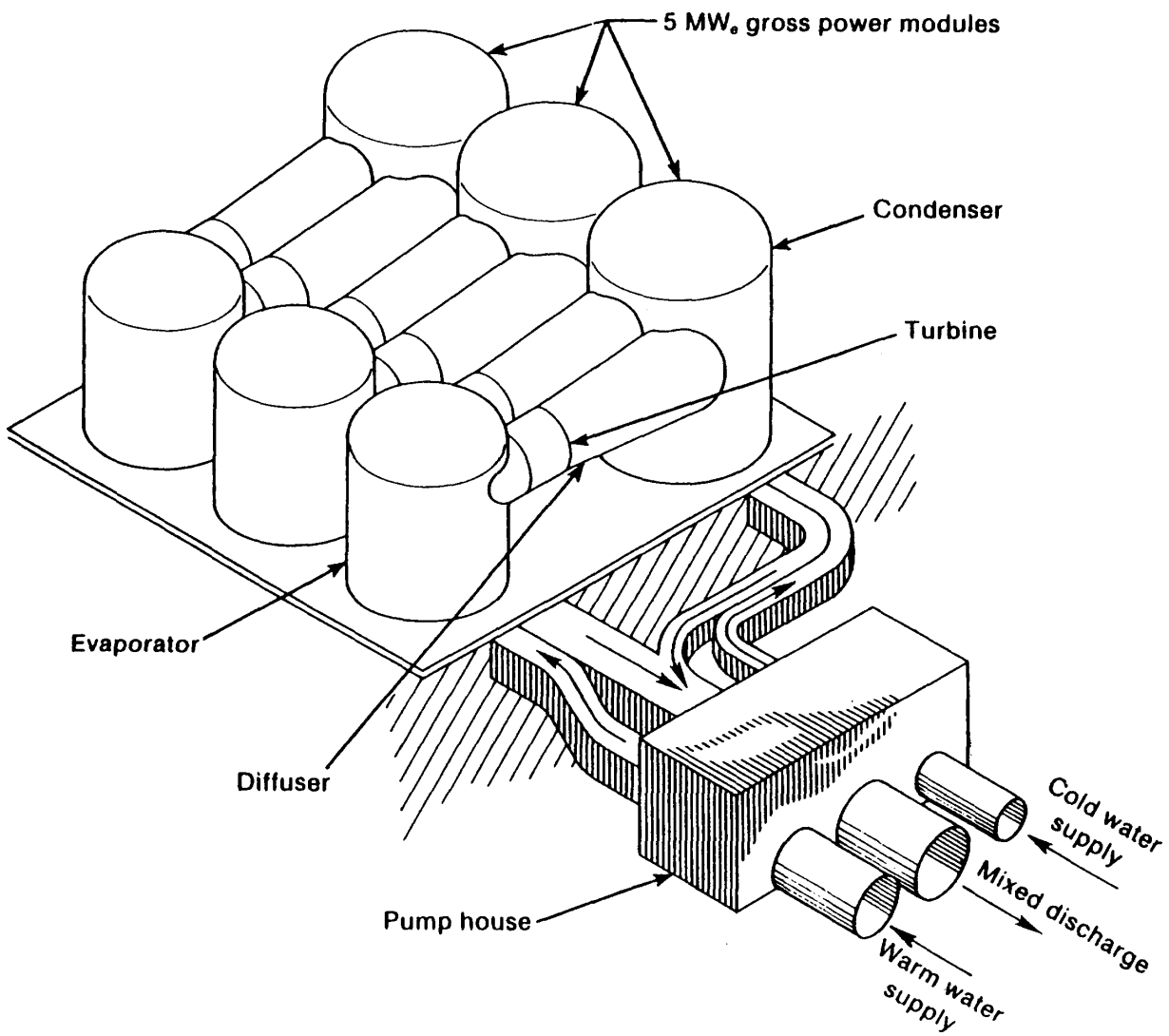

Figure 1-1. Conceptual design for a three-module, 10-MW, open-cycle OTEC plant

The system analysis and cost-goal projections of the Federal Ocean Energy Technology Development Program are shown in Table 1-1. They indicate that significant reductions in the cost of the turbine/generator system will be required to bring OTEC plant costs to a range where OTEC can be an important alternative to the nuclear and fossil-fired plants currently in use.

The size of the low-pressure stage of a conventional turbine has reached the limits of practicality, because of the tooling cost associated with larger blades. To achieve national program goals, it will be necessary for the OTEC research community to examine a technology alternative and techniques for larger power plants that can significantly reduce the cost and increase the power output of an OTEC turbine/generator set. A proposed objective is a 60%

Table 1-1. OTEC System Cost Goals

Total System Projected Capital Cost ($/kW$_e$)		
Current Technology (closed-cycle)	Interim Goal (five-year)	Long-Range Goal
$9680	$7200	$3200

Subsystem Projected Capital Cost ($/kW$_e$)					
	Current Technology	Interim Target (five-year)		Long-Range Target	
Subsystem	Closed-Cycle	Closed-Cycle	Open-Cycle	Closed-Cycle	Open-Cycle
Power system	$4120	$3200	$2900	$1500	$1280
Building and structure	560	400	670	290	670
Seawater system	5000	3600	3630	1410	1250

cost reduction from $2500/kW to $1000/kW for the turbine/generator. Because the design of the turbine will affect the design and cost of other power-plant components, it may be more useful to define the objective in terms of reducing the total plant cost to $3200/kW [7].

There are at least four ways to approach reducing the first costs of an open-cycle OTEC power plant through innovative turbine design and construction:

- Increase the output of the turbine by achieving higher steam throughput or conversion efficiency, or both.
- Decrease the cost of the turbine by using innovative materials or innovative turbine configurations.
- Increase the size of the turbine.
- Decrease the cost of the system by innovative, cost-effective integration of the turbine into the system.

Because energy costs are determined by operating costs, innovative techniques must also enhance equipment life and the maintenance characteristics of the power plants.

1.2 Technical Objective

The technical objective of this study is to identify and evaluate turbine system design concepts that significantly reduce the cost of electricity from an open-cycle OTEC plant. The concepts are directed at systems in the 2-5 MW_e range, with a cost goal of $1000/$kW_e$ for the turbine/generator system.

This objective is stated in terms of the turbine cost. However, a valid approach in meeting this objective could involve performance or cost credits against other subsystems incurred because of reduced performance requirements

or simplified hardware interface designs, made possible by the design or operating characteristics of the turbine concept.

1.3 Task Description

The Federal Ocean Energy Program has undertaken conceptual design studies to define a turbine for open-cycle OTEC system feasibility experiments based on the application of proven, low-risk technologies. As a complement to this activity, three university research teams completed feasibility evaluations of innovative turbine concepts that could significantly reduce system costs but that may represent higher development risks and uncertainty. The approach involved six steps:

1. Establish the expected performance of the baseline system [a single-flow rotor using 1.32-m (52-in.) blades on a 104-in.-diameter disk].
2. Conceive alternative turbine configurations that address and appear to satisfy the project objective.
3. Analyze the alternatives and select a preferred approach based on the criterion of maximum impact on system cost.
4. Specify the physical configuration of the turbine based on aerodynamic, thermodynamic, and structural requirements.
5. Evaluate the band of uncertainty and technical risk associated with the configuration selected and define the minimum research required to address those issues.
6. Document the design with sketches, specifications, and a technical report that provides a backup analysis and rationale.

Section 2.0 describes the projections and supporting rationale for performance and cost limits that can be expected if design methods and materials currently employed in the turbine industry are used. Faculty and student teams from the Massachusetts Institute of Technology (MIT), the University of Pennsylvania, and Texas A&M University proposed three alternative innovations described in the body of this report. Section 3.0 describes the work done by the MIT team under the direction of Prof. A. D. Carmichael in defining and evaluating several cantilevered turbine concepts that utilize simple, two-dimensional blades fabricated from plastic composite materials. The team from the University of Pennsylvania, under the direction of Prof. N. Lior, evaluated a vertical-axis orientation of an axial-flow turbine using blading produced with composite plastic blading. This work is described in Section 4.0. Section 5.0 describes the design and performance of a single-stage and a two-stage dual-flow, radial inflow turbine configuration. This work was completed by a student team from Texas A&M University, under the direction of Prof. T. Schobeiri. In Section 6.0, we provide a summary and discussion of all the study results and suggest a research path that could achieve the performance and cost goals established for the technology.

2.0 THE BASELINE DESIGN

2.1 System Design Criteria

Defining open-cycle OTEC system operating parameters involves an analysis of the performance and cost interactions of the major subsystems shown in Figure 2-1. The trade-off that must be made is between conditions that balance the gross power delivered from the turbine/generator against the power consumed in the system to operate the warm- and cold-water seawater pumps and the gas evacuation compressor required to prevent a buildup of desorbed air and maintain suitable pressure in the system.

The seawater temperatures typical of tropical Pacific islands such as the Hawaiian Islands are approximately 26°C warm water and 6.5°C cold water [8]. Numerous studies conclude that the steam conditions at the inlet and outlet of an OTEC turbine that provide maximum power output are in the following ranges [6]:

Inlet temperature	22.0-23.0°C
Inlet pressure	2.61-2.77 kPa
Outlet temperature	9.5°-11.1°C
Outlet pressure	1.17-1.3 kPa

All turbine concepts have been evaluated at operating conditions that fall within the ranges above.

2.2 Baseline Turbine Design

As a point of reference against which to evaluate the innovations identified in this study, we selected a baseline turbine/generator design, cost, and performance description based on the use of existing blading and rotor hardware. The starting point for a baseline definition is the L-1 stage of a nuclear turbine (for example, the Westinghouse WBB 381). A CREARE study [6] showed that the blade geometry of this stage, when matched with a new nozzle design, would operate at reasonable efficiency under OTEC conditions and produce 1.2-1.4 MW_e. However, the industry is able to produce a longer blade. This existing hardware is not yet suitable for OTEC applications because of the blade angles, but it could be redesigned for an OTEC turbine. Because of its larger geometry, this turbine could deliver 2.0 MW, according to a simple scale-up of the CREARE results. This scaled-up projection based on existing L-1 blade performance has been defined as the baseline turbine of this study. There is good reason to believe that this turbine blading could be built by using existing design and construction methods, and result in the largest open-cycle OTEC turbine practical using existing technology.

As part of its definition of baseline system performance, a study team from MIT completed an additional analysis to define the performance potential of this blade and wheel technology if the blading were redesigned for optimum performance at the OTEC conditions previously described. The thermodynamic and aerodynamic analysis of the optimum baseline axial-flow turbine was based on the Soderberg method for loss prediction, with additional terms added to account for tip clearance and wetness losses. Second-order polynomials were used to represent the steam properties in the turbine. The design was carried

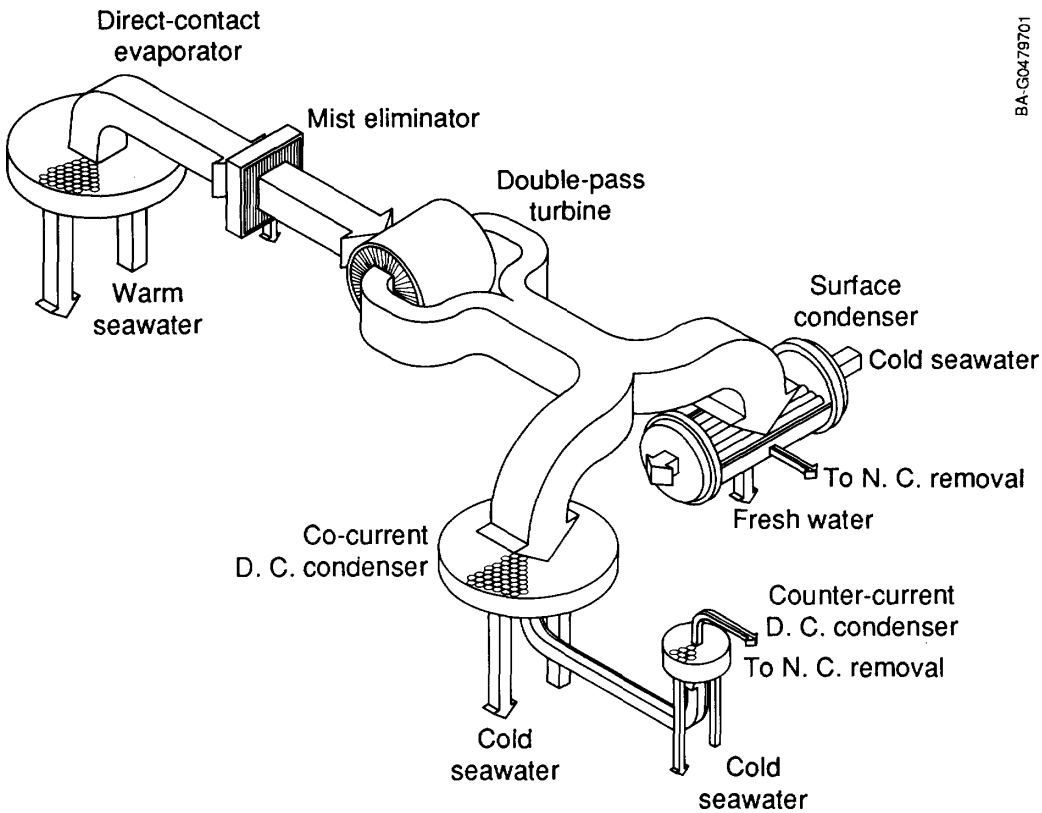

Figure 2-1. Major subsystem schematic for open-cycle OTEC

out using mid-radius blade conditions, and the flow conditions at the hub and tip were then determined using the free-vortex model. The design process used the criterion of reaction greater than zero at the hub.

While the simple radial equilibrium analysis was adequate to characterize the performance of the turbine, the final design should accommodate spanwise variations in a full radial equilibrium model. It was assumed that there is no pressure recovery in the downstream diffuser (as in all the studies described in this report).

2.3 Baseline System Design Variations

Using the method and results described above, it is possible to examine the baseline axial-flow turbine, defined as a scale-up of the CREARE design to 1.32-m (52-in.) blades, as well as variations on this design. In the context of cost reduction, it is instructive to focus on two designs--one that optimizes the power output and another that optimizes the conversion efficiency of the turbine. Table 2-1 shows the operational parameters for each of these designs. Note that the "high-power" design has considerably lower efficiency but still produces more power because of the increased mass flow rate.

Table 2-1. Performance Characteristics of Baseline Axial-Flow Turbine Optimized for High Efficiency and High Power Output

	High Efficiency	High Power
Power (MW)	1.74	2.39
RPM	1200	1200
Efficiency (total-static) (%)	77	64
Mass flow (kg/s)	21.7	35.9
Nozzle angle (mid-radius)	72°	60°
Exit flow angle	-20°	-2°
Hub reaction (%)	6.2	7.7
Tip speed (m/s)	332	332

The cost of this axial-flow turbine and the other components of the OTEC power plant was estimated from information provided by the Solar Energy Research Institute (SERI) turbine consultants. The baseline turbine is estimated to cost $2 million (±20%), and the associated generator system is estimated to have a unit cost of $145/kW plus a fixed cost of $0.85 million for switch gear. For the 2.0-MW baseline system, the turbine/generator system should cost approximately $3.6 million. In terms of cost per unit power output, the combined turbogenerator system is estimated at approximately $1800/kW.

An important feature of this turbine cost estimate is the breakdown of the costs by components. The study methodology relies heavily on this breakdown to identify the most promising of the turbine components as targets for cost reductions. The turbine cost was divided among the major components of the 2.0-MW axial-flow turbine from estimates by the turbine consultants, as shown in Table 2-2. This breakdown shows that the turbine blading (including the nozzle blades) and the turbine casing are the prime targets for cost reductions. This is to be expected, particularly for the blading, because the baseline axial-flow turbine has very long, highly twisted rotor and nozzle blades that are expensive in terms of both material and fabrication costs.

Table 2-2. Breakdown of Turbine Costs for 2.0-MW Baseline, Axial-Flow Design

Category	Percentage
Rotor blading	26
Casing	24
Disk and shaft	15
Bearings and lube system	6
Valves and piping	8
Other (includes nozzle blades)	21
Total	100

The cost of the remaining OTEC system components was estimated assuming that the turbogenerator system in the baseline configuration represents roughly one-third of the total OTEC system cost. The balance of the system cost (about one-half of which is related to the cold-water supply) was assumed to be proportional to the square root of the mass flow rate (water) through the system. The accuracy of this assumption is limited to reasonable variations in the flow rate, so only systems with mass flow rates between 20 kg/s and 40 kg/s were considered (the 2.0-MW baseline turbine has a mass flow rate of 27 kg/s).

Applying this estimate of total system cost to the axial-flow turbine provides an interesting contrast between the baseline 2.0-MW design and the high-efficiency and high-power designs described in this section. Table 2-3 shows the actual costs and unit costs estimated for each version of the axial-flow system. The table indicates the economy of scale in the turbine and the total system. The high-power design increases the mass flow rate (steam) by 33% over the baseline design, but the unit turbine cost drops by 15% and the unit system cost drops by 8%. The table also demonstrates the misleading nature of turbine efficiency as a design parameter: the high-efficiency design not only does not improve on the baseline system, it increases the unit turbine cost by 13% and the unit system cost by 9%. The underlying assumption here is that the rotor diameter is limited to the current industry practice for the LP stage rotor, a 1.32-m (52-in.) blade length.

2.4 Discussion of Results

There appear to be opportunities to significantly reduce the cost of steam turbines using the existing (or baseline) technology. Beginning with a design that uses existing blading technology with a turbine/generator output of 2.0 MW_e and a cost of approximately $1800/kW, it is reasonable to project an increase in the power output to 2.4 MW and a reduction in the cost to $1530/kW.

Table 2-3. Costs of Systems Using Conventional Axial-Flow Turbines

System	Percentage	Cost (M$)	$/kW
Baseline system (2 MW)			
Turbine/generator	35.3	3.6	1800
Balance of system	64.7	6.6	3300
Total	100.0	10.2	5100
High efficiency (1.74 MW)			
Turbine/generator	36.7	3.6	2040
Balance of system	63.3	6.2	3520
Total	100.0	9.7	5560
High power (2.39 MW)			
Turbine/generator	32.4	3.7	1530
Balance of system	67.6	7.6	3190
Total	100.0	10.2	4720

However, a 1% loss in efficiency necessitates a $150/kW increase in the balance-of-system cost over that of the efficient turbine, so that the net effective turbine/generator cost would be $1680/kW. This is still higher than the technology cost goal of $1000/kW determined to be necessary to achieve cost-effectiveness.

The analysis of the axial-flow turbine provides information upon which to base the innovative design process. In particular, Tables 2-2 and 2-3 suggest the most promising areas for cost reduction. As mentioned, Table 2-2 indicates the predominance of the blading and casing in the cost of the turbine. Therefore, the two primary goals of the innovative turbine design will be (1) simplification of the turbine blades in both the materials required and the fabrication process, and (2) simplification of the turbine casing and integration of this casing with the evaporator and the condenser. Table 2-3 indicates an additional incentive toward higher-power turbines, because these would take advantage of economies of scale in power system costs. Any turbine that could easily be expanded to higher power production without major additional costs would thus be advantageous.

The analysis of the baseline axial-flow turbine demonstrates the advantage of a higher power output in terms of unit turbine and system costs. From this analysis, we may conclude that the most obvious and most conservative improvement to the OTEC turbine system would be a slight modification of the conventional axial-flow design so the turbine operates at its highest mass flow rate and power output, which this study shows to be 35.9 kg/s and 2.39 MW, respectively. This simple improvement provides a 15% reduction in the unit turbine cost and a more than 7% reduction in the unit system cost.

3.0 THE CANTILEVERED BLADE DESIGN

3.1 Introduction

A team from MIT examined the possibility of cantilevered blade construction as a turbine wheel construction option. This approach is embodied in three different configurations: radial inflow, radial outflow, and crossflow. All three configurations utilize a simple, two-dimensional blade that lends itself to low-cost materials and fabrication processes. Each of these wheel configurations offers interesting possibilities for efficient integration into an OTEC system, because the steam flow path and form factors permit effective interfaces with other system components. The radial outflow configuration also offers the potential for integrating a compact diffuser section, should one prove feasible.

3.2 Radial Cantilevered (Squirrel-Cage) Design

For the purpose of this study, possible variations on squirrel-cage turbines are divided into two categories: radial-inflow turbines and radial-outflow turbines. The basic arrangement of these turbines is shown in Figure 3-1. Both types use rotor blades that are cantilevered from a central disk. The radial-inflow turbine has fully supported nozzle blades just outside the rotor blades; the radial-outflow turbine's nozzle blades are cantilevered from the casing just inside the rotor blades. All these blades have a uniform cross section along their lengths, and with careful aerodynamic design, this cross section can be made the same for the rotors and the nozzles.

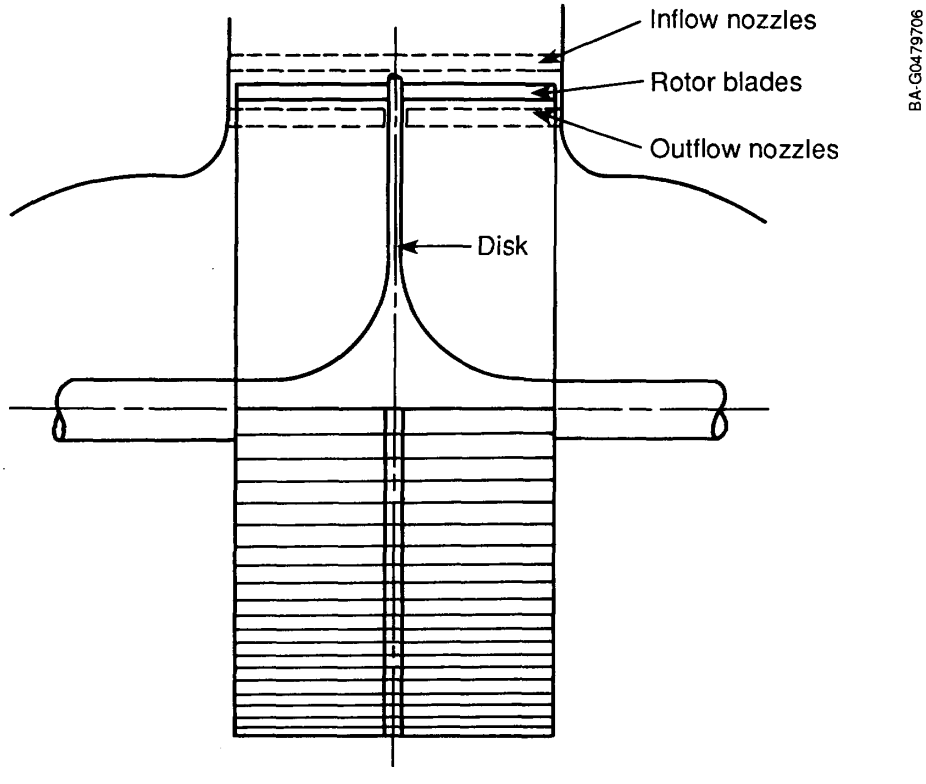

Figure 3-1. Radial-outflow and radial-inflow squirrel-cage turbine

The performance of these turbines was analyzed by using a one-dimensional flow model that is a slight modification of the method used for the baseline axial-flow turbine analysis. The method must be altered to allow for variations in the rotor blade radius and the flow area across the rotor blade. The resulting operational parameters for radial-inflow and radial-outflow turbines are shown in Table 3-1. These parameters show that the conversion efficiencies of these turbines are fairly high and the tip speeds are not too large (i.e., not supersonic).

After these operational characteristics were established, the maximum expected blade stress was estimated. This maximum stress will occur in the rotor blades, since they are subject to both aerodynamic and centrifugal loading. For steel rotor blades (density, ρ, ~7900 kg/m^3; allowable stress, σ_{max}, ~340 MPa) and composite rotor blades (ρ ~1500 kg/m^3; σ_{max} ~340 MPa), the maximum allowable blade length between ring supports was determined for the cantilevered configuration shown in Figure 3-1. With steel blades, the maximum length between supports is approximately 0.39 m, and with composite blades it is 0.89 m.

A general analysis of these squirrel-cage turbines indicates the possible benefit of reduced blading fabrication costs. These configurations seem to have two disadvantages, however, and both are related to the combination of radial and axial flow inherent in the design. First, it is awkward to collect the radial steam flow (for the radial-outflow turbine) or disperse the radial steam flow (for the radial-inflow turbine) around the circumference of the rotor. This difficulty may lead to the need for a large, complicated casing, and integration of the turbine with the evaporator and condenser may be difficult. Second, the axial flow into or out of the turbine is limited by the radius of the rotor. This limitation, coupled with the limits on the length of the rotor blades caused by stress considerations, restricts the power output of the turbine. This effect is more pronounced in the radial-inflow version, because the steam flow along the rotor shaft is less dense than it is in the radial-outflow turbine.

Table 3-1. Performance Characteristics of Radial-Outflow and Radial-Inflow Turbines

Element	Outflow	Inflow
Power (MW)	1-3.5	1-2
RPM	1200	1200
Efficiency (total-static) (%)	70-76	70-76
Nozzle angle	60°-70°	60°-70°
Reaction (%)	50-70	50-70
Rotor diameter (m)	4.3	4.3
Maximum rotor width (m)	1.9	1.1
Tip speed (m/s)	270	270

In summary, squirrel-cage turbines offer possible benefits in terms of reduced blading costs, but they seem to present expensive complications in terms of the turbine casing and the integration of the turbine with the evaporator and the condenser. No detailed cost analysis was completed because of a decision to apply limited time and resources to the analysis of another type of turbine which was inspired by the work on the radial-flow turbines, namely, the crossflow turbine.

3.3 The Crossflow Turbine Design

The crossflow turbine is essentially a two-stage, partial-admission, radial-flow turbine. Each stage uses rotors in a semicircular arrangement. The first stage acts as a radial-inflow design and the second stage acts as a radial-outflow design. The unique aspect of the crossflow configuration is that both these stages employ the same rotor blades, which are mounted around the circumference of the rotor disk, and the connection between the stages is nothing more than flow across the cylindrical space formed by the rotor blades. A cutaway view of this arrangement is shown in Figure 3-2.

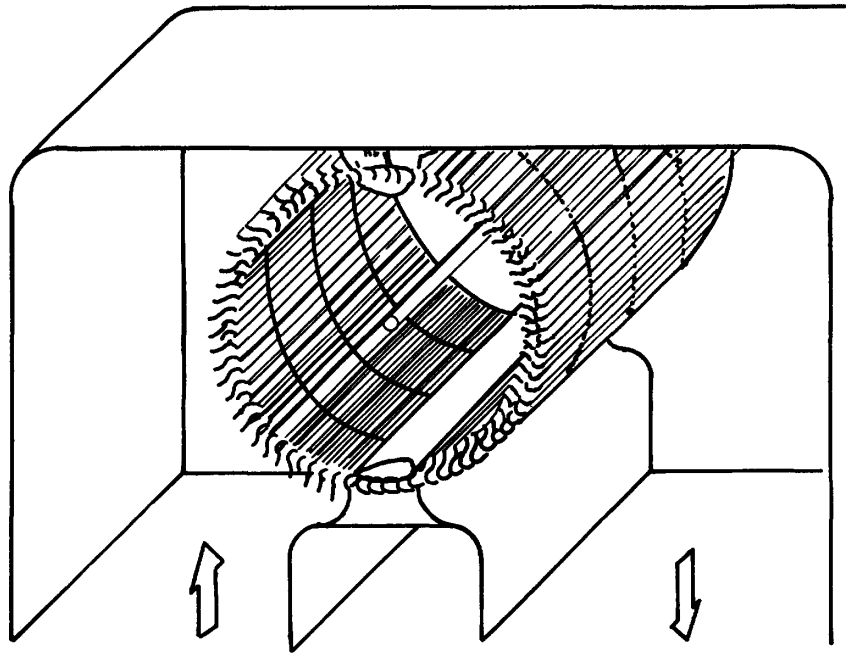

Figure 3-2. The crossflow turbine: cutaway view

It is important to note that this design is a slight modification of the standard crossflow turbine that has been described in the past and has found particularly advantageous use in low-cost hydroelectric systems. The modification involves adding second-stage nozzle blades, located just inside the rotor blades and supported at both ends by means of an additional bearing in the rotor disk. This arrangement is shown in Figure 3-3. The second-stage nozzles allow a more even distribution of the turbine energy conversion across the two stages, which improves the overall efficiency of the design.

3.4 Crossflow Turbine Performance Analysis

Aerodynamic and thermodynamic analyses of the crossflow turbine are complicated by the interdependence of the two stages. The design was accomplished

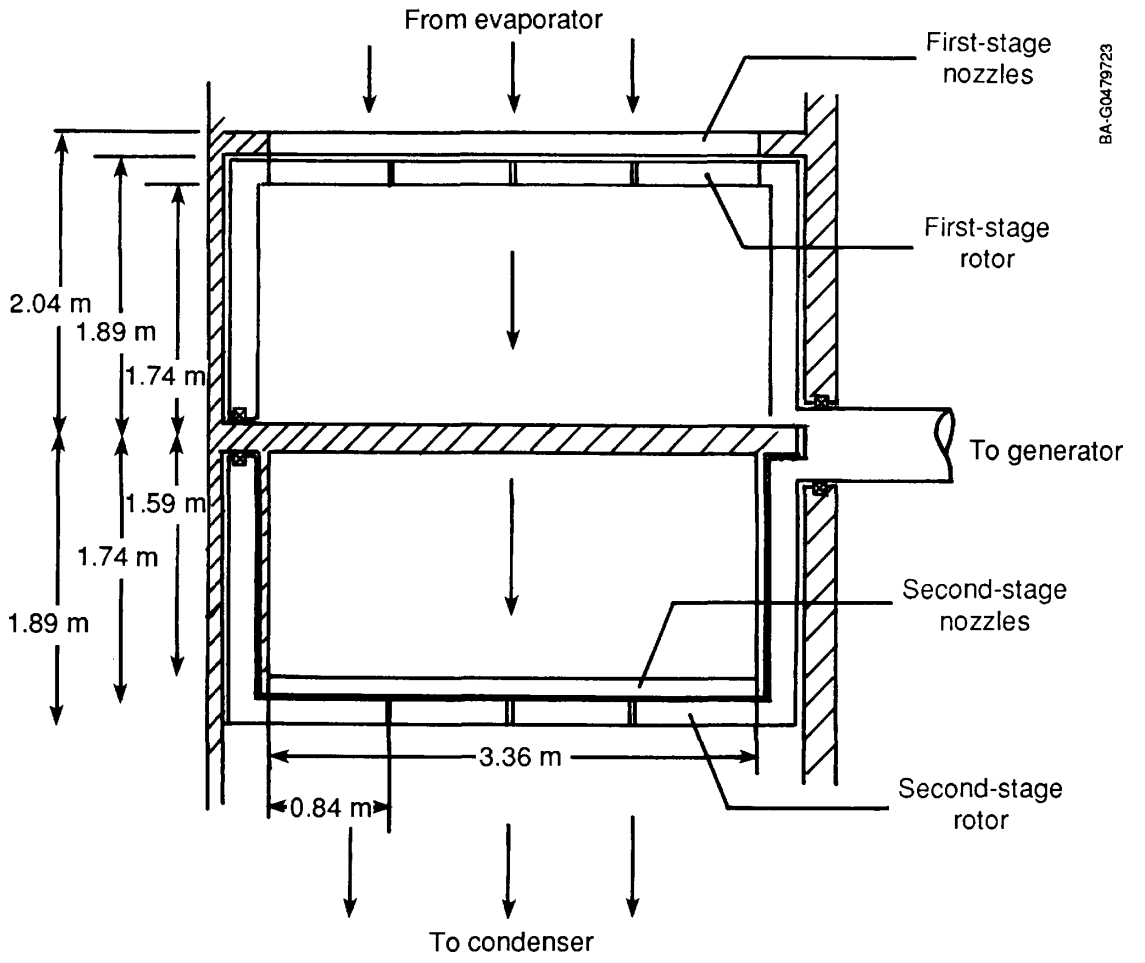

Figure 3-3. Arrangement of the crossflow turbine, showing second-stage nozzle blades and additional bearing

by adapting the method described above to analyze the squirrel-cage turbines. The first stage is treated as a radial-inflow turbine and the second is treated as a radial-outflow turbine. The design optimization of each stage is performed in an iterative fashion until all coupled parameters match (including rotor blade angles, radii, and spacing; mass flow rate; and steam properties in the center of the rotor). An additional term is included in the loss calculation to account for the partial admission configuration of each stage. Table 3-2 shows the results of this design process. The rotor width has been set to produce 2.4-MW output for comparison with the high-power version of the axial-flow turbine.

The necessity of using each rotor blade twice, in opposite directions, leads to a symmetrical impulse blade design with a uniform cross section. The impulse design and the two-stage configuration result in a greatly reduced blade speed, as shown in Table 3-2, which in turn reduces blade stresses. This reduced stress permits innovative, very inexpensive rotor blade materials and fabrication methods to be used. The rotor blade's construction is shown in Figure 3-4. Cold-rolled steel sheet is used to form the basic blade curve, and injection-molded plastic fillers are used to complete the blade cross section. A stress analysis of these blades indicates that they must be supported approximately every 0.84 m. If this support is in the form of retaining rings, as shown in Figure 3-3, the width of the rotor is readily expanded to permit high mass flow rates.

The major uncertainty in a performance analysis of the modified crossflow turbine is the nature of the flow within the turbine, as the steam passes from the exit of the first-stage rotor to the leading edge of the second-stage nozzles. As a first-order approximation, we may consider that the pressure at the exit of the second stage will be kept uniform by the condenser conditions imposed, and the pressure drop across the second-stage nozzles will be fairly high, all of which would be expected to impose an approximately uniform radial flow at the leading edge of the second-stage nozzles. If these nozzles are designed to have radially directed leading edges, the losses from this source could be assumed to be negligible. Figure 3-5 shows this expected flow pattern through the midrotor section of the crossflow turbine.

To test this concept, a simple model of the center section of the crossflow rotor was constructed and a water test was run. The model has vanes along the incoming semicircle that produce the expected swirl in the flow at the exit of

Table 3-2. Performance Characteristics of the Crossflow Turbine

Power (MW)	2.4
RPM	600
Mass flow rate (kg/s)	31
Efficiency (total static)(%)	77
Nozzle angle (1st stage, 2nd stage)	70°, 65°
Rotor diameter (m)	3.78
Rotor width (m)	3.8
Tip speed (m/s)	119

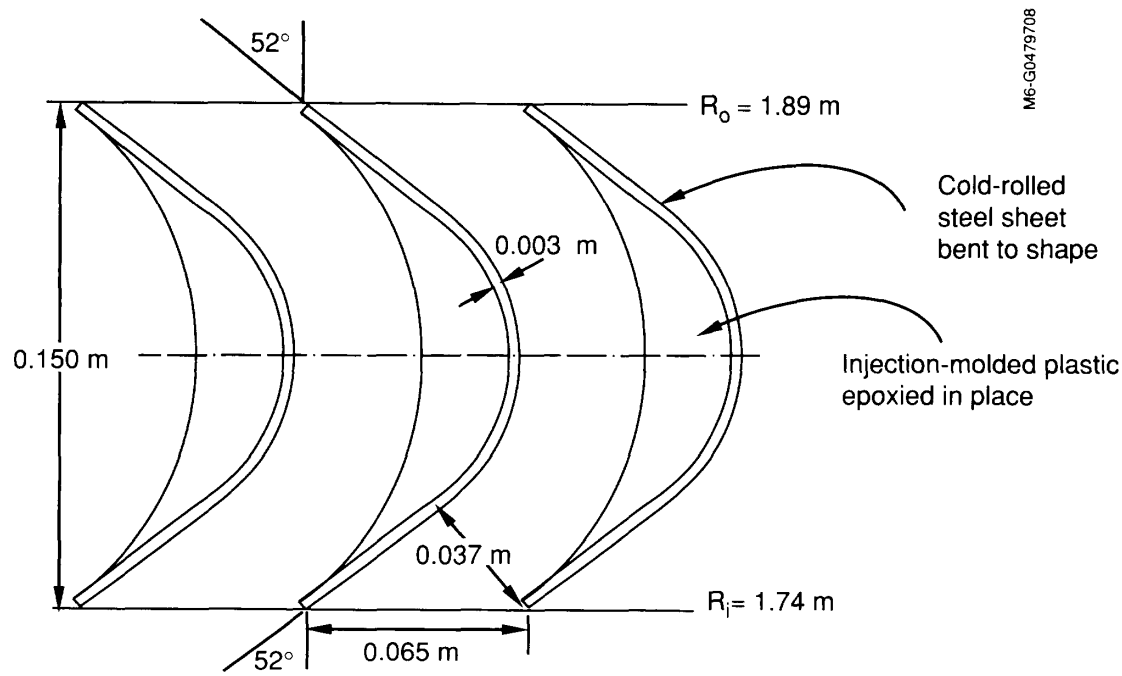

Figure 3-4. Construction of the rotor blades for the crossflow turbine

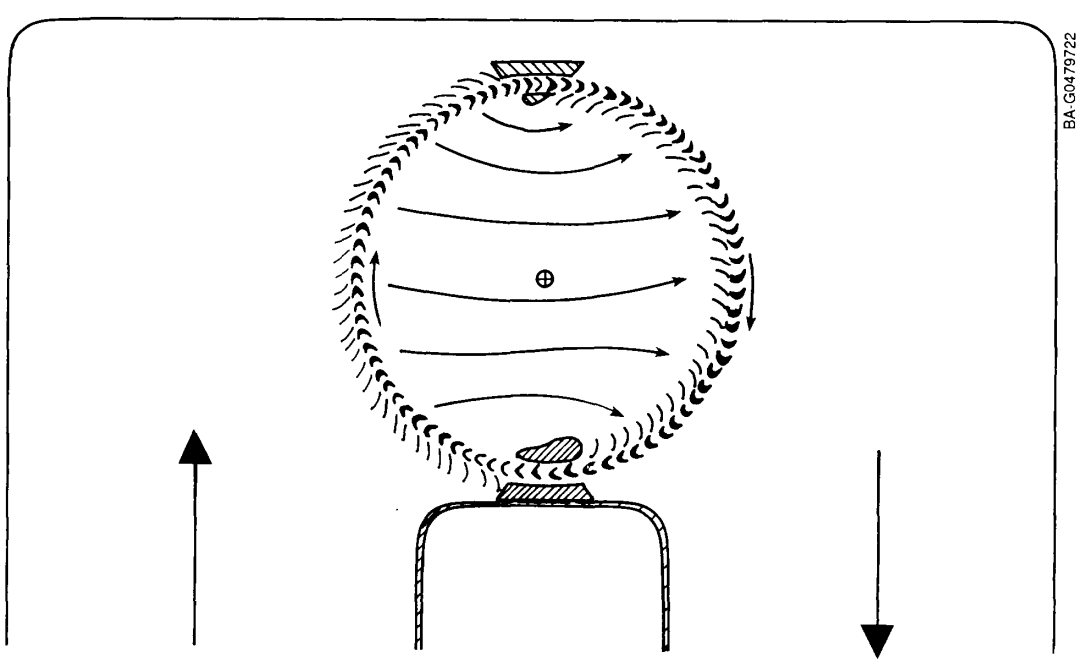

Figure 3-5. Flow pattern expected through the crossflow turbine

the first-stage rotor. Several layers of thick screen are used to disperse water from the inlet reservoir evenly along this semicircular first stage. The model also has blades along the outgoing semicircle that approximate the second-stage nozzle blades, with radially directed leading edges and enough turn to produce the design input flow to the second-stage rotor. To visualize the flow in the center of the rotor, researchers attached a thin black thread to each of the inlet vanes and allowed it to follow the dominant streamlines coming off that vane. Photographs of the operating experiment show that streamlines curve through the center of the section, as expected from the swirl of the incoming flow, but they disperse radially on approaching the second-stage nozzle blades. A few nozzle blades on each end of the second stage encounter nonradial flow at incidence, but even these could be designed for minimal loss by orienting them in the actual incidence direction demonstrated by the water test.

3.5 Cost Analysis

To estimate the cost of the crossflow turbine, we may begin with the cost estimates for the baseline system and identify the type and magnitude of the changes in the estimate for the crossflow system. The main cost savings center in the turbine blading, which was assumed to consist of equal portions of material and labor (fabrication) costs. The major element of the material cost of the crossflow blades is the cost of the steel sheet, which may be assumed to be proportional to the weight of the steel. The crossflow blades are longer than the axial-flow blades, but the cross section of the steel portion is much smaller, so the total weight is about one-third of that for the axial-flow turbine. The cost of the fabrication of the blades will be proportional to the time required and the complexity of the operations. The simple bending and injection molding required for the crossflow blades is estimated to cost about one-tenth that of the detailed milling process required for the highly twisted, axial-flow blades. This results in a total cost for the crossflow turbine blades of about one-fifth that of the axial-flow blades. The other savings component lies in the simplified rectangular casing of the crossflow turbine, which is estimated to cost approximately one-half that of the axial-flow casing.

If these cost reductions are incorporated into the cost estimate of the axial-flow turbine, the result is a significant reduction in both the absolute and unit cost of the turbine and the total power system. Table 3-3 shows the resulting cost estimates for the crossflow system and compares this system cost with that of the best axial-flow design (the high-power version). The crossflow design used in this comparison has the same power output as the high-power, axial-flow design (2.4 MW).

An analysis of the modified crossflow turbine yields encouraging conclusions. Table 3-3 indicates that the crossflow turbine does not quite satisfy the goal of a $1000/kW unit turbine cost, but it comes fairly close at $1087/kW and represents an improvement of 28% over the high-power, axial-flow system and 38% over the baseline (20-MW) axial-flow system. Unit system costs are similarly decreased by 13% and 20% over the high-power and baseline axial-flow turbines, respectively, to a value of about $4100/kW. The design is also amenable to extension to higher power levels without modification; thus, even greater cost reductions are possible for a larger power system based on the crossflow design.

Table 3-3. Predicted Costs of Crossflow Turbine and System and Comparison with High-Power, Axial-Flow Turbine

Crossflow Component/ System	Cost (M$)	Percent of High-Power, Axial Flow Turbine System
Blading	0.18	20
Casing	0.29	50
Other turbine	0.94	100
Generator	0.35	100
Switch gear	0.85	100
Total turbogenerator	2.61	72
Balance of system	7.10	93
Total system	9.71	87

3.6 Conclusions and Recommendations

Attempts to use innovative design techniques to produce dramatic cost reductions have identified a modified crossflow turbine design as a promising approach. Analysis of this turbine shows a reduction of 38% in the unit turbine cost and a reduction of 20% in the unit system cost, compared with those of the baseline axial-flow system. At a $1087/kW unit turbine cost, the crossflow turbine comes close to meeting the design goal of $1000/kW. These results suggest that the modified crossflow turbine should be seriously considered as a low-cost alternative to the conventional axial-flow turbine. More specifically, we recommend that the following steps be taken to continue the development of the crossflow turbine as a viable OTEC option:

- The technical uncertainty of the new crossflow design should be examined by constructing a scale model of the turbine and subsequent testing with air as the working fluid.
- The details of the crossflow turbine fabrication should be examined, particularly in relation to the materials and methods available for fabricating the blading.
- The possibility of lengthening the crossflow rotor should be pursued to take advantage of economies of scale in reducing the turbine and system unit costs.

4.0 THE VERTICAL-AXIS, AXIAL-FLOW CONFIGURATION

4.1 Introduction

A student research team from the University of Pennsylvania directed by Prof. N. Lior evaluated the feasibility of an alternative steam turbine design configuration originally proposed by Westinghouse (Figure 4-1). This turbine configuration consists of a single-flow, single-stage turbine mounted on a vertical shaft. The use of innovative materials in the construction of the turbine blades was also examined. The high-strength, lightweight materials under consideration are composite structures of fiber-reinforced plastics and urethane foams. The main advantages of this design include space efficiency in terms of overall system integration, easy application to larger designs, resistance to corrosion and fatigue, and lightweight (as well as low-cost) rotor and rotor support construction.

The Westinghouse concept for open-cycle OTEC [5] consisted of a 140-MW_e gross single-flow axial turbine mounted in an ocean-based platform. The concept included several innovative features:

1. A large, vertical-shaft, low-speed turbine
2. An annular housing incorporating the major components of the open-cycle OTEC power plant
3. Use of innovative materials in the turbine blading and in the pressure vessel.

The results of these three innovations are volume efficiency in component packaging and lower cost than conventional construction.

The steam conditions for open-cycle OTEC permit the use of innovative materials and concepts that are not applicable to conventional steam turbines. The Westinghouse concept utilized a large, vertical-axial-flow turbine 44.5 m in diameter with 12.2-m-long blades. This turbine had a low speed of rotation, only 200 rpm. Blades of this size cannot be built using conventional metal technology because of sag and stress limitations. The blades proposed are almost 10 times larger than the largest existing blades. However, fiber-reinforced plastics and composites have been used successfully in military helicopter applications in blades approximately 12 m long.

Mild OTEC steam conditions also permit a simplification of the highly expensive, complex, high-pressure housing usually associated with steam turbines. Westinghouse proposed using a special formulation of commercially available, high-density reinforced concrete. This concrete has relatively low air infiltration rates and can be cast to a very smooth surface finish without polishing. The concrete is used in pressure-vessel construction for the liquid natural gas (LNG) tanks aboard LNG tankers. The use of reinforced concrete necessitates curved surfaces, and the annular structure meets this criterion.

The annular arrangement accommodates the area required for the flash evaporators inside the outer ring of the pressure vessel. Normally, the area of the steam passage is increased as the vapor rises from the evaporation region to enhance elimination of carry-over droplets. This results in a

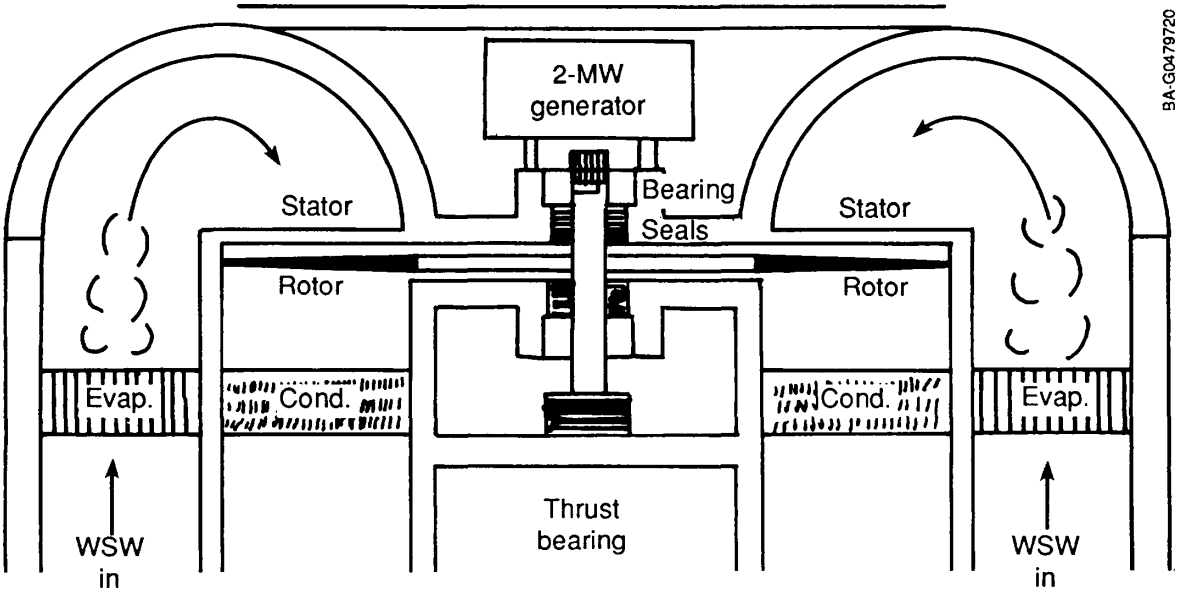

Figure 4-1. 2-MW_e open-cycle OTEC concept

complex vessel shape for a horizontal-shaft (conventional) turbine and uneven flow symmetry at the turbine inlet. However, it is easy to incorporate area increases in a vertical, annular design. The annular design also allows steam-flow redistribution to take place. This results in a uniform flow of steam as it enters the vertical-shaft turbine. The power plant vacuum enclosure is a major cost contributor. According to a rough calculation, an annular arrangement of flash evaporators, turbine, diffuser, and condensers results in a volume usage of about 80% compared with that of a conventional horizontal layout for a 2-MW_e turbine.

For these reasons, design efforts centered around the Westinghouse concept. The specific disk speed and disk size were confirmed by manual calculations for the Westinghouse turbine. These quantities were used to find the dimensions and rotational speeds of geometrically similar axial turbines of 2- and 5-MW_e designs. Root stresses were calculated for the two modules and found to be nearly the same. A complete mechanical design was carried out on a 2-MW_e module. Since the stress loading is nearly the same as that of the design scale-up, many of the mechanical specifications for the 2-MW design are also applicable to the 5-MW_e module.

4.2 Design Analysis

In designing a turbine, there are many factors to consider in addition to the system configuration. The blades must be designed and examined from the standpoint of aerodynamics, stress, and ease of manufacturing, and the mechanical peripherals, such as seals, bearings, shaft, and connections, must be studied and designed. The University of Pennsylvania team adopted a systems approach to attend to each of these considerations in sufficient depth to create a total, workable turbine design.

The first stage of the project was a critical review of the work done by Westinghouse [9,10]. The correctness of the assumptions and changes made by Westinghouse had to be ascertained before its design could be scaled down. The next step was to scale down the Westinghouse design to meet this project's goals, which dictated that the turbine must have an output of 2-5 MW and a construction cost less than or equal to $1000/kW.

4.2.1 Scaling Analysis

Essentially, the scaling operation entails designing an entirely new turbine. The blade shape, bearings, housing, and choice of materials may all have to be completely changed, for maximum efficiency in the smaller size. The changes necessary were determined through a series of mathematical analyses.

The design of the turbine follows the steps suggested by Balje [11]. The first steps include determining the characteristic disk size (D_s) and the characteristic rotational rate (N_s). The input variables for these dimensionless variables include the efficiency of the Westinghouse turbine and the adiabatic head associated with the entry and exit conditions of the turbine. The diameter and rotational speed of the scaled-down turbine were determined by the use of the variables above. The mass flow rate, volumetric flow rate, and velocity through the turbine were also determined. Table 4-1 shows a comparison of the original Westinghouse design with scaled vertical-shaft turbines operating under the conditions specified in this project. The first column contains the specifications of the original design study by Westinghouse for a 140-MW turbine. The second column contains the calculated specifications for a 140-MW turbine of the same dimensions operating at the slightly different conditions specified here. The specifications for this turbine as scaled down to 2 and 5 MW are given in the third and fourth columns.

4.2.2 Fluid-Flow Analysis

After the scaling analysis was completed, detailed aerodynamic, vibrational, and stress analyses of the scaled-down design were completed. These analyses were coupled, because the pressure distributions resulting from the fluid-flow model are used as input to the structure model that determines stress concentrations and natural frequencies.

Two finite-element programs were used in the analysis of the turbine blades. FLUENT (version 2.81) is a computer program designed by CREARE, Inc. [12], for the modeling of fluid flow; it uses a finite-difference numerical procedure to solve the Navier-Stokes equation. The team used FLUENT to optimize turbine blade efficiency by modifying the blade geometry and orientation until a favorable (decreasing) pressure gradient was obtained. The FLUENT program can handle a variety of fluid regimes, which includes laminar turbulent, steady, subsonic, and single-phase fluid flows. It can also accommodate the effects of two-phase flow, gravity, and buoyancy.

Table 4-1. Comparison of Vertical-Axis, Axial-Flow Turbine Designs

Westinghouse Design (140 MW) (English Units/SI Units)[a]	Modified Design (140 MW)[b]	Scaled-Down Turbine (2 MW)[b]	Scaled-Down Turbine (5 MW)[b]
Inlet pressure			
0.406 psi/2.799 kPa	2.758 kPa	2.758	2.758
Inlet temperature			
73.3°F/22.4°C	22.5°C	22.5°C	22.5°C
Inlet enthalpy			
1094 Btu/lbm/2545 kJ/kg	2437 kJ/kg	2437 kJ/kg	2437 kJ/kg
Inlet entropy			
2.055 Btu/lbm°R/8.6039 kJ/kgK	8.6094 kJ/kgK	8.6094 kJ/kgK	8.6094 kJ/kgK
Outlet pressure			
0.183 psi/1.26 kPa	1.24 kPa	1.24 kPa	1.24 kPa
Outlet temperature			
50.75°F/10.41°C	10.23°C	10.23°C	10.23°C
Outlet enthalpy (isentropic)			
1049 Btu/lbm/2440 kJ/kg	2437 kJ/kg	2437 kJ/kg	2437 kJ/kg
Outlet moisture (isentropic)			
3.3%/3.3%	3.3%	3.3%	3.3%
Outlet specific volume (isentropic)			
1605 ft^3/lbm/100.2 m^3/kg	106 m^3/kg	106 m^3/kg	106 m^3/kg
Rotational speed			
200 rpm	200 rpm	1670 rpm	1057 rpm
Tip diameter			
146 ft/44.5 m	44.5 m	5.313 m	8.4 m
Isentropic enthalpy drop			
44.98 Btu/lbm/104.6 kJ/kg	105.84 kJ/kg	105.84 kJ/kg	105.84 kJ/kg
Mass flow rate			
1.31×10^7 lbm/hr/1651 kg/s	1633 kg/s	23.33 kg/s	58.32 kg/s
Characteristic disk diameter, D_s			
literature: 2.0	Calculated: 1.96		
Characteristic disk speed, N_s			
literature: 0.24	Calculated: 0.232		

[a]Quantities calculated for original Westinghouse test conditions.
[b]Quantities calculated for inlet/outlet conditions specified for this project.

ANSYS (version 4.3) was developed by Swanson Analysis Systems, Inc. [13], to solve various engineering problems. For this project, ANSYS was used to determine the stress concentrations and natural frequencies that would result from the pressure distribution resulting from fluid flow through the turbine. The pressure and force distributions were inputs for ANSYS to perform vibrational and stress analysis. The main variables for the ANSYS analysis consisted of different blading materials.

4.2.3 Vibrational Analysis

Vibrational analysis is a significant part of turbine analysis. Prior knowledge of the resonant frequencies of the turbine design allows us to alleviate the potential for damage. The divergent oscillations that result from resonance could cause a turbine blade to fail because of material fatigue from excessive vibrations and would certainly reduce blade efficiency. Unanticipated oscillations could do damage to the housing of the turbine and thus could compromise the low-pressure atmosphere of the inlet steam. These hazards can be avoided if the relevant natural frequencies of a particular blade design are known. Through the analysis of existing designs, and with the aid of further computer analysis, the goals can be reached.

The Westinghouse turbine design was chosen as a baseline model because the literature on its design was the most readily available. The Westinghouse design and analysis were directed to avoiding three types of dynamic response: flutter, twist-up, and modal response.

Flutter is the absorption of flow energy caused by blade deformation and vibration. This type of response would reduce the efficiency of the system as well as cause blade structural fatigue. After a significant amount of research on this type of vibration, Westinghouse concluded that a swept-forward spar design reduces the possibility of classical flutter. The swept-forward spar design moves the mass center in front of the aerodynamic center, thereby creating a righting couple that balances the beam. This sort of dynamic mass overbalance is effective because only a small fraction of the blade's total mass is moved forward to the leading edge and there is little effect on other types of vibrations or the force exerted on the disk by centrifugal forces.

Twist-up is caused by the torsional deformations caused by loads imposed from the steam flow and centrifugal forces. The degradation in performance that can be caused by these types of deflections from the steam flow is avoided by canting the blade in the direction opposite of the twist caused by steam loading, so that during operation the blade would be twisted to a position that provides the most optimal blade geometry. Twist-up caused by centrifugal forces is obviated by using the box spar, which centralizes the mass distribution within the blade.

The bending vibrations caused by modal response are prevented by designing the turbine so that the angular velocity would not correspond to an integral multiple of an individual blade's natural frequency. A graph of the natural frequencies of these modes versus the turbine rotational speed was expressed by Westinghouse as a Campbell diagram (Figure 4-2). From this diagram, designers found that the two lowest modes were potentially dangerous.

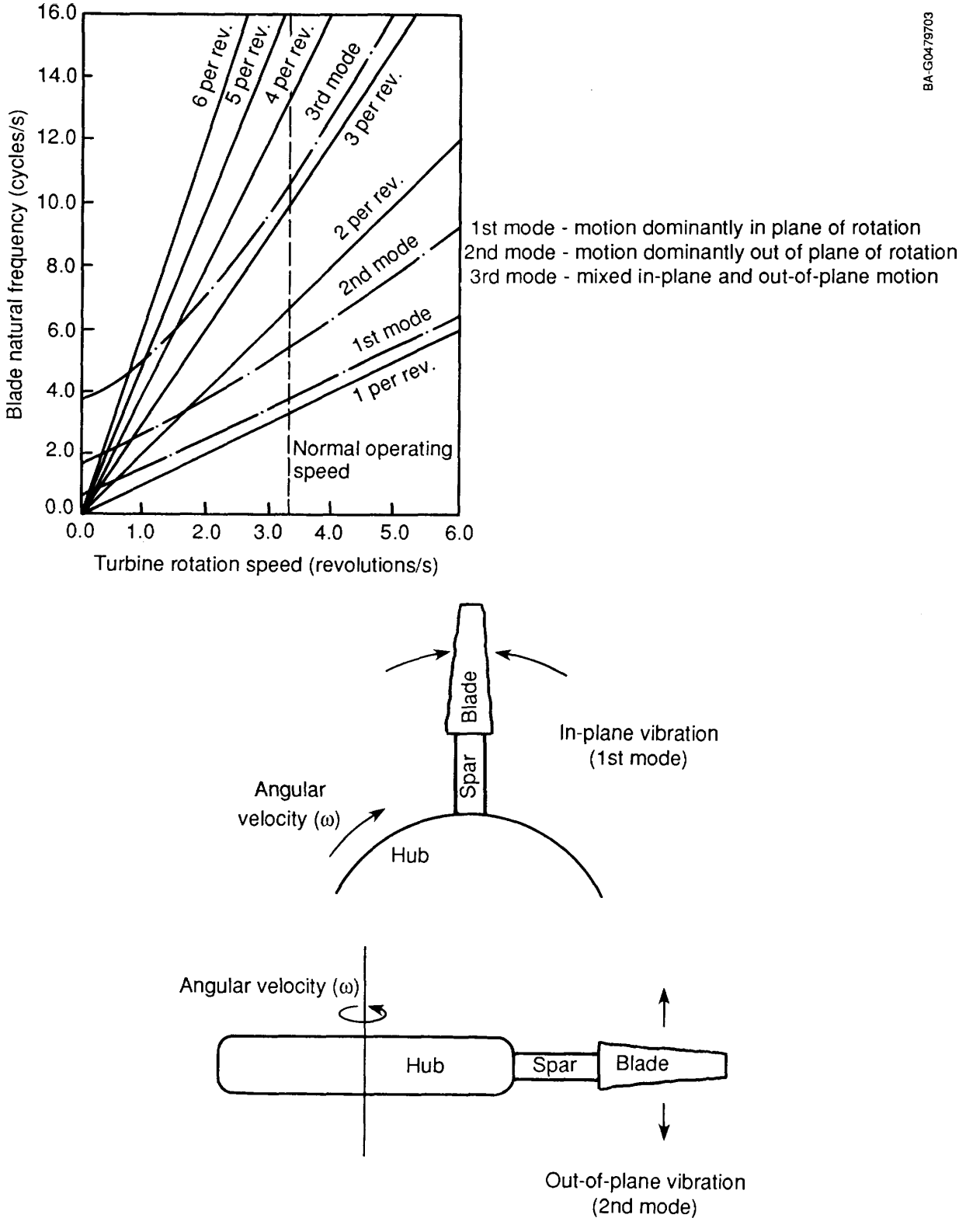

Figure 4-2. In-plane vibration (first mode) and out-of-plane vibration (second mode)

The second mode of vibration is a result of vibration that occurs normal to the plane of rotation. It is potentially dangerous because it could couple with the disk and result in an interactive blade-disk, backward-wave, "wheel" mode. Researchers believe that large-scale internal damping, which is accomplished by using a composite disk material, should suffice in keeping such vibrations to a minimum.

The fundamental mode of blade bending vibration is consistently greater in frequency than the one-cycle-revolution excitation at normal operating speeds. It consists mainly of in-plane vibration and is sufficiently close to once-per-revolution excitation that varying steam flow rates due to inlet flow distortions could excite a vibrational response. Varying rates of steam flow could excite this type of vibration to a moderate response. Care must be taken to ensure that such steam flow distortions are accounted for in the design and mitigation steps are taken as required.

4.2.4 Stress Analysis

Stress and strain are expected to be much smaller in this model than in the original Westinghouse turbine, permitting less expensive materials to be used than those required by the greater stresses in the larger turbine. Using ANSYS, researchers obtained stress plots for stresses due to centrifugal and steam flow loads. These stresses influence the choice of materials.

Other factors influencing the choice of materials for all parts of the turbine are fatigue, creep, and reaction to the environment. Fatigue affects the blades and all other moving parts of the turbine; creep affects all parts of the turbine. Both influence the life cycle cost of the turbine. Some parts of the turbine are exposed to a marine seawater environment, because of water droplet carryover from the evaporator, and all of them must stand up to the low pressures produced by the vacuum. Since the OTEC facility is expected to function for several decades, replacement of parts over time must be figured into the cost of maintaining the facility. Fouling on the blades caused by the salt, minerals, and marine organisms found in the seawater flowing through the facility can also reduce efficiency and must be removed periodically. All these factors must be analyzed to maximize the efficiency and safety of the turbine over its expected lifetime.

Although good indicators were generated in this study, the results of the fluid flow and structural analyses were inconclusive because of model limitations that were not overcome in the project's time frame. Performance and structural conclusions in this study are based on extrapolation of the results of the Westinghouse study.

4.3 Mechanical Design

4.3.1 System Arrangement

The turbine in this conceptual configuration is placed in a toroidal casing, and the generator is in a separate chamber above (Figure 4-3). The housing consists of a series of concrete shells that may be removed one by one to access various subsystems of the power plant. This will allow for both modular construction and ease of maintenance.

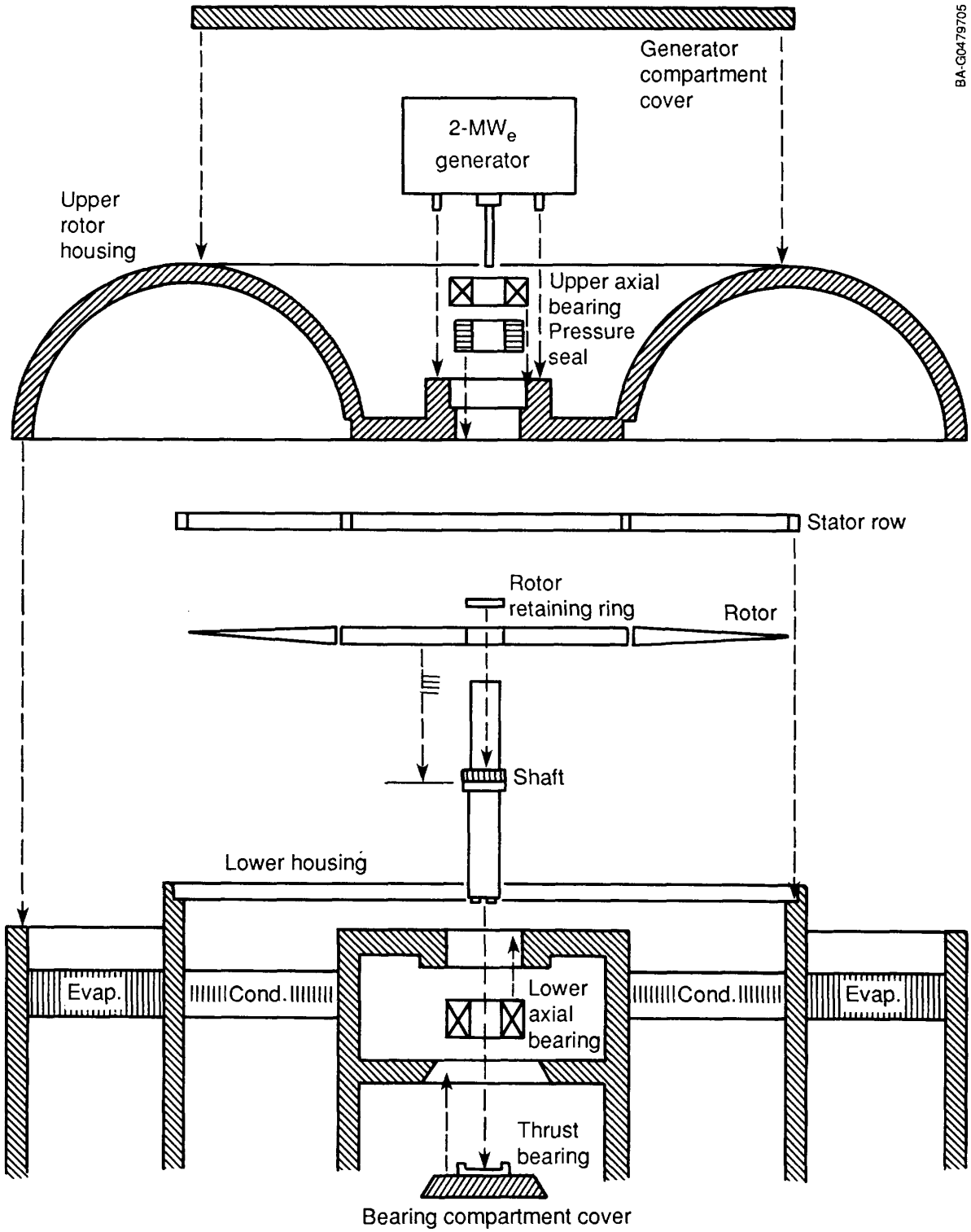

Figure 4-3. Axial turbine housing: exploded view

4.3.2 Rotor Design

The mechanical construction of this turbine consists of 120 blades attached to a central hub (Figure 4-4). To reduce weight, a hollow box spar made of fiber-reinforced plastic is extended from the root of the blade to the rim of a central disk with a smaller diameter than the 2.64-m disk in the baseline. Not only does this reduce the overall mass of the system, it considerably reduces the cost of construction by promoting ease of assembly. The individual blades are maintained in their positions by spacer blocks placed between each spar. A thin, Fiberglas fairing is attached above and below this composite hub to eliminate pressure loss through the spaces between the spars.

4.3.3 Blade Design

The blade design in this study is based on scaled results from blade profiles developed by Westinghouse in its original studies (Figure 4-5). The two profiles reported by Westinghouse were first scaled to the correct chord lengths of 13.20 cm and 11.56 cm established in the scaling analysis. Then the profiles of four other intermediate cross sections were created by using linear interpolation between these two scaled profiles. The profiles were then canted to their correct angle of attack by using a graph of gauging (Figure 4-6) developed by CREARE [6].

The blade design is estimated to be 81% efficient. Each blade is 132 cm long, with a root chord of 13.20 cm and a tip chord of 11.56 cm. This results in a

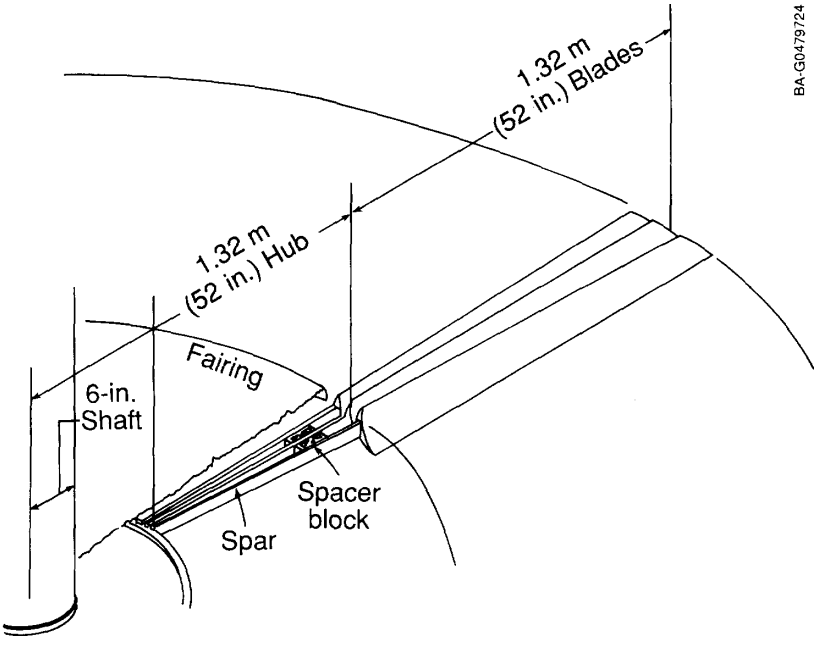

Figure 4-4. Axial turbine rotor construction

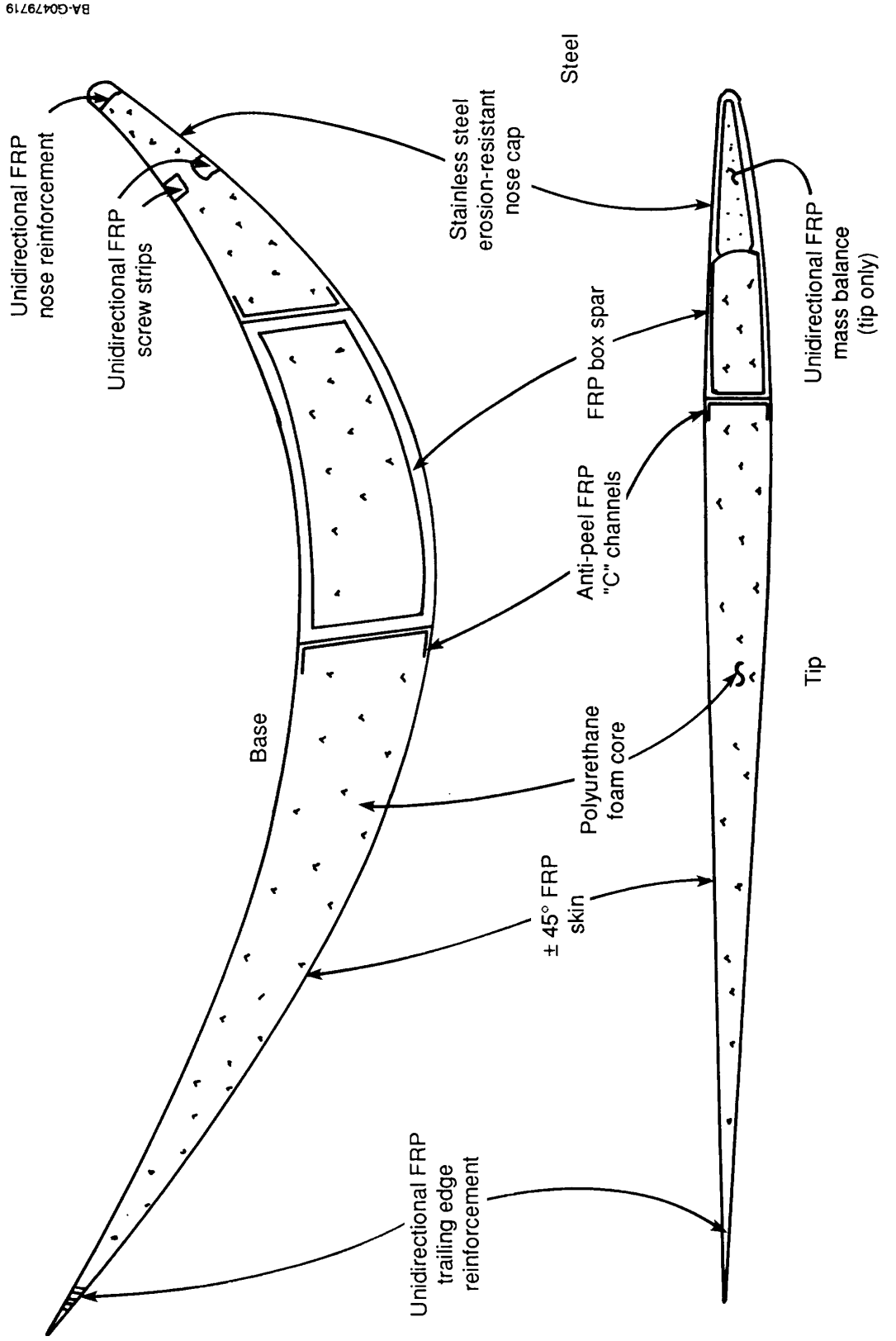

Figure 4-5. Typical axial turbine rotor blade construction

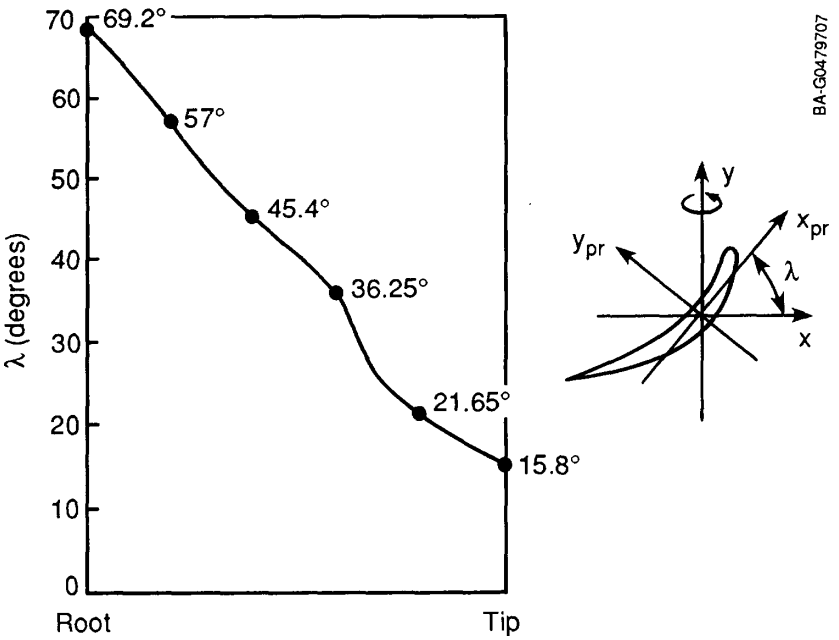

Figure 4-6. Axial turbine blade: λ vs. blade station

chord ratio of 0.88. Each blade consists of a urethane core embedded within an E-glass shell. An internal box spar runs the length of the blade to provide stiffness. The spar sweeps forward from the mass center of the root to the leading edge of the tip. This helps reduce flutter by placing the mass center ahead of the aerodynamic center of the blade. The spar extends 81 cm from the root of the blade in the direction of the center of rotation, providing a point of attachment to the central hub. Each blade weighs 1.15 kg, which results in a total weight of 138 kg for the 120 blades in the turbine rotor.

4.3.4 Central Hub and Shaft Design

The central disk of the rotor is not a single piece. It consists of a 102-cm-diameter central hub of 440A stainless steel to which is attached the 81-cm spar extensions from each blade. The spars are separated by a spacer block bolted between each pair of blades. Covering both the top and bottom of the disk is a Fiberglas fairing that keeps pressure loss through the disk to a minimum.

The hub is a biconal disk of 440A stainless steel. In cross section, the disk is 5.8 cm thick at the shaft and 1.78 cm thick at a point just behind the rim. The rim is shaped to allow the blades to be attached with a hinge and pin arrangement. The hub has 16 internal splines to facilitate attachment to the shaft. The total weight of the central disk was estimated to be approximately 227 kg.

The shaft supports the turbine rotor and transmits torque to the generator. The shaft was designed to be lightweight and to resist bending and torsion. It provides a platform for hub attachment as well as support for the bearings and seals. To eliminate transfer of thrust from the generator to the rotor bearings, the shaft-to-generator connector consists of a 16-spline arrangement configured to slide under the load.

The outer diameter of the shaft is 30 cm. This is a standard tubing size and provides a great enough girth to prevent buckling. The thickness of the shaft wall, 0.5 cm, was determined by applying the maximum shear stress formulae and a torque transmission of 6705 Hp (5 MW). This design will carry the torque produced with a safety factor of 2.86.

4.3.5 Bearing and Seal Design

The use of a vertical shaft presents novel problems in the design of bearings for support. Most turbomachinery makes use of hydrodynamic journal-type bearings to support the turbine shaft, but most, if not all, turbines are built with a horizontal shaft [14,15]. The downward force supported by the thrust bearing was estimated to be equal to the weight of the rotor and shaft when at rest plus a force determined by the area of the blading multiplied by the difference between the inlet and outlet pressures when turning at maximum speed. For design purposes, the radial forces were estimated to be two-thirds of the thrust forces.

The bearings must resist an approximate thrust load of 2672 kg and a radial load of 1782 kg. Two arrangements of bearings were studied. The first was a hydrodynamic bearing, with one thrust bearing below the shaft and journal bearings placed above and below the rotor. A second, promising arrangement called for roller bearings. The Torrington Company was consulted about that but its recommendations were not received in time to be included in this report. Design and performance data of selected bearing designs are summarized in Table 4-2. Using very conservative assumptions, the team concluded that the bearings would consume 52 kW, or less than 2% of the total power produced.

The housing design proposed requires only one seal. This seal is located between the upper axial bearing and the generator housing, and it is of the labyrinth type. This noncontact seal allows some steam leakage but creates little or no friction. The generator housing is maintained at atmospheric pressure. This effectively prevents steam leakage into the generator housing. The following formula was used to calculate the leakage rate:

$$G = 25\ KA\ \{P_i/V_i\ [1 - (P_o/P_i)^2]/[N - \ln\ (P_o/P_i)]\}^{1/2}\ ,$$

where

G = leakage rate ($in.^3/s$)

K = flow coefficient (60 to 120 for straight-through seals)

A = clearance area between shaft and seal ($in.^2$)

P_i = upstream pressure (psi)

V_i = upstream specific volume ($in.^3/lb$)

Table 4-2. Vertical-Axis Turbine Bearings Design and Performance Data

Type	Kingsbury Tilting-Pad
Outer diameter	30 cm
Inner diameter	20 cm
No. of pads	12
Pivot point	58% from leading edge of pad
Minimum film thickness	0.004 cm
Temperature rise	4.5°C
Oil flow	3277 cc/s
Power loss	32 hp (23.9 kW)
Type	Tilting-Pad
No. of pads	8
Diameter	20 cm
Diameter clearance	0.061 cm
Length	10 cm
Temperature rise	0.56°C
Oil flow	442 cc/s
Power loss	10 hp (7.46 kW)

P_o = downstream pressure (psi)

N = number of labyrinth stages.

The value for the distance between the shaft and the blades of this seal are commonly taken to be 0.02 times the shaft diameter. Four chambers were chosen, and the shape of the blades was taken from the general guidelines provided in the Mechanical Components Handbook [16]. The thermodynamic values were taken from tables. The leakage rate was calculated by using the higher value of K, and a value of 0.000295 m^3/s was obtained. The throughput of the turbine was calculated by multiplying the mass flow rate by the specific volume of the input steam. The value obtained for the throughput was 2540 m^3/s. From this, we see that the leakage flow is negligible. Since the clearance is extremely small, the seal is designed to float on the shaft and therefore to be self-aligning. Its integration with the turbine shaft, bearings, and spline coupling is shown in Figure 4-7.

4.4 Materials

Several criteria influence the selection of materials. First, the material must have a high tensile strength in order to withstand the stresses caused by the extremely rapid rotation of the turbine (465 m/s tip speed). Because the blades should not deform appreciably under operating stresses, the Young's modulus, stress/strain, should also be high. Also, to minimize stress due to inertial loads, the material should not be unduly heavy.

Temperature tolerance is a minor factor in the material's selection. The molding method proposed by Westinghouse entails shaping the fiber-reinforced plastic directly onto the urethane rigid-cell foam core. If this molding method is retained, the material must be workable at a temperature well within

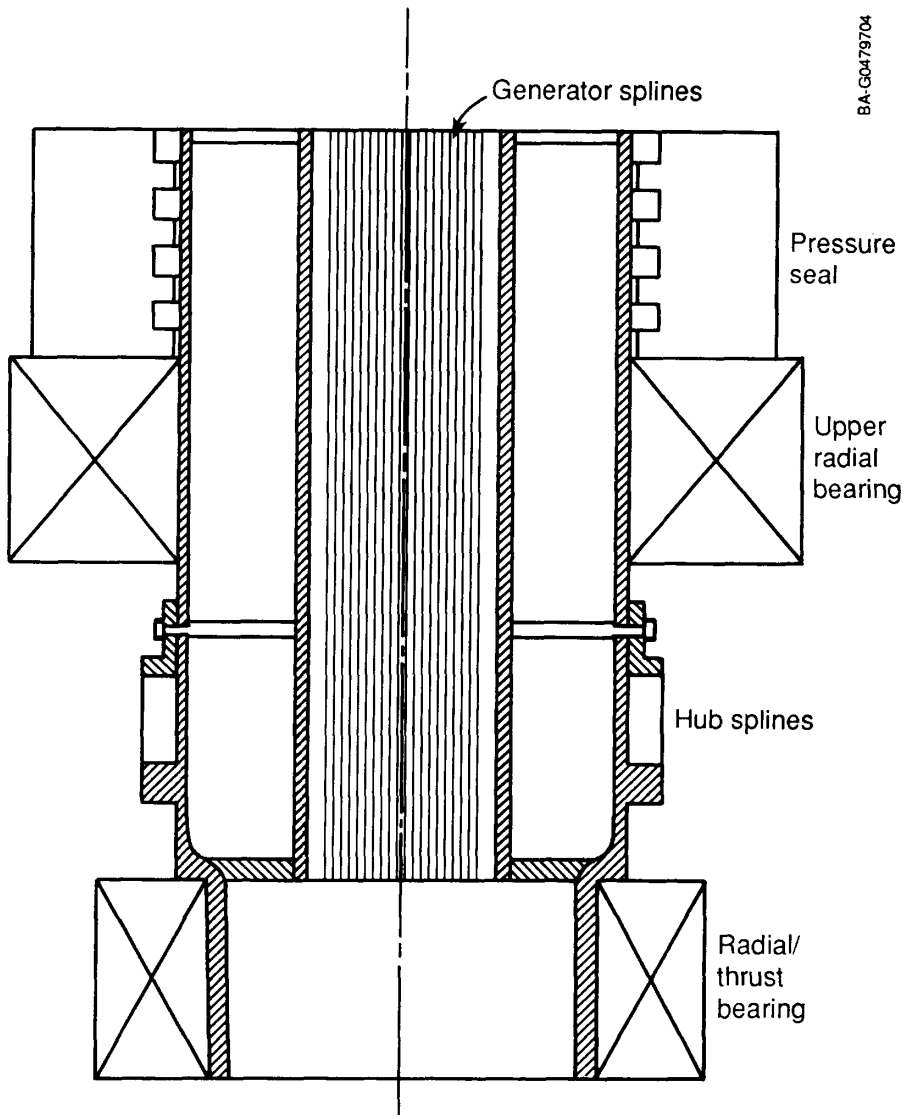

Figure 4-7. Axial turbine central shaft bearing/seal placement

the foam's tolerance. All of the fiber-reinforced plastics under consideration are capable of withstanding the relatively low temperatures used in the OTEC turbine.

The choices made by Westinghouse were used to provide baseline numbers for purposes of comparison. The E-glass fiber selected by Westinghouse is one of the most commonly used, general-purpose reinforcement fibers. The fibers are used to reinforce an epoxy base material.

Our research has yielded several viable materials for the blade shell and spar. Properties of some of the most attractive of these are shown in Table 4-3 [17].

Table 4-3. Properties of Candidate Materials

Material[a]	Young's Modulus	Ultimate Strength	Density	Poisson's Ratio
E-glass	41 GPa	1035 MPa	1.97 g/cm^3	0.3
S-glass	52 GPa	1690 MPa	1.65 g/cm^3	0.3
Carbon	183 GPa	380 MPa	1.54 g/cm^3	0.3
Kevlar-49	46 GPa	650 MPa	1.40 g/cm^3	0.3
Graphite	131 GPa	1575 MPa	--	0.3

[a]E-glass (E for electric) is the most commonly used, all-purpose fiber reinforcement. It is also the cheapest of the materials listed, but fairly brittle. S-glass (S for strength) is stronger but more expensive than E-glass and also somewhat brittle. There are several types of carbon fibers available, designed for high strength, high modulus, ultrahigh modulus, etc. Kevlar is the trade name for Aramid and is manufactured by Dupont. The newest version is Kevlar-149, for which we do not have data. Kevlar is much tougher than E- or S-glass. There are several variants of graphite fibers available, suitable for different uses.

Undirectional fibers are used to form the spar, which must be especially strong, but cross-ply fibers may be used for the blade shell, to provide strength in several directions. Other factors influencing the strength of fiber-reinforced plastcs are the uniformity of the fiber orientation and the number of defects. Further research must be done, however, on the cost of the materials. The final choices must be based on mechanical properties and temperature tolerance versus cost considerations.

An inexpensive, rigid-cell urethane foam, which has low moisture absorption, forms the core of the turbine blade. Since weight is a less important factor in the hub design, 440A stainless steel is used for the hub and shaft. If steel were used for the blades, each one would weight about 11.36 kg, instead of about 1.15 kg for the composite construction, and hub stresses would increase greatly.

4.5 Cost Analysis

The cost of the turbine described in this section is difficult to define precisely because the design was not completed. However, some trends can be observed if we make a few simplifying assumptions. If the cost of the turbine is directly related to the weight of the materials used, using composite plastic blading is likely to reduce the weight and cost of the turbine rotor up to 25 times (455 kg versus 11,365 kg for a steel wheel). However, much of the turbine's cost is connected with the turbine enclosure, and the University of Pennsylvania team estimated that a system configuration built around a vertical orientation of the turbine axis can reduce the enclosure cost as much as 80%. If these factors are combined, researchers estimate that the Pennsylvania design would weigh less than half that of the baseline configuration and, therefore, be proportionally less expensive.

The design proposed uses composites that are more expensive than steel, but the forming processes are much cheaper. A mold for the blade's urethane core will last indefinitely, whereas metallic blades require replacement of both forging dies and the cutting tools used for final finishing.

Conventional plants include the cost of a casing. This vessel usually has to withstand high temperatures and pressures. The casing for an OTEC plant can be made of cheaper materials, such as concrete, that are also easier to shape.

The design and development cost of a new turbine rotor can be in the range of several million dollars. This represents a significant cost, which would have to be recovered against the selling price of the system hardware. Until the total system design is completed, an accurate cost analysis cannot be determined. Thus, this analysis provides only a rough order-of-magnitude estimate.

4.6 Conclusions and Recommendations

Preliminary results indicate that a vertical-axis turbine configuration of the type proposed here can be utilized to produce 2 MW of gross power. The design approach is sound; however, the software that was available to the team was not the most suitable for modeling the turbine. The scaling analysis of previously reported Westinghouse results provides an excellent definition of design and thermodynamic performance parameters. However, a confirmation of these preliminary results with analyses using closely coupled finite-element models for fluid flow, stress, and dynamic response, at a grid geometry sufficient to capture the geometry and flow features, is required to verify the analysis in this project. The FLUENT computer program was limited in terms of the size and complexity of the flow region being modelled. Also, it was difficult to model the unique properties of fiber-reinforced plastics with the available ANSYS program. There are several programs and enhancements to PATRAN-based, finite-element programs that overcome the many difficulties encountered with ANSYS [18]. We recommend that this initial work be used as a basis for future study, with an emphasis on satisfactorily modelling turbine blade behavior.

It was not possible to complete a suitable cost modelling activity in this project. A valid assessment of the innovation requires quantification of the turbine cost and a more complete definition of the turbine's interfaces with other plant subsystems. Future work should address these elements and focus on the preferred power size, because it appears that there may be cost benefits associated with turbines that are even larger than those identified in this study.

5.0 A MIXED-FLOW TURBINE WITH RADIAL INFLOW

5.1 Introduction

A team from Texas A&M University described and analyzed the performance of a mixed-flow turbine blading configuration with radial inflow of steam and exhaust along the axis of rotation. This type of blading is most often seen in gas compressors rather than in turbines. A notable exception is the turbocompressor found in many vehicle power plants. It is not used in utility applications because of the complexity of the staging required for the pressure ratios found in conventional steam plants. The OTEC application does not involve large pressure ratios across the turbine; therefore, this approach may have much more relevance for OTEC than for conventional plants.

OTEC thermodynamic boundary conditions indicate that the turbine component does not undergo significant thermal and structural stresses or fluid mechanical loading. Because the isentropic enthalpy difference for these conditions is constant, the turbine power is determined entirely by the turbine's mass flow and efficiency. Assuming that we have the highest available turbine efficiency, achieving a reasonable turbine power in commercial operations requires high mass flows. For low-pressure and high-mass-flow operation, the axial design concept is a common application, where low-pressure stages with high-efficiency blades are used (e.g., ASEA Brown Boveri, Kraftwerk Union AG, and Westinghouse). The CREARE design report [4] shows that, for a turbine power of 10 MW, the preferred design for the axial turbine has an outer diameter of 14.4 m with a blade length of 4.3 m. This is a solution that leads to the need for an extremely large enclosure geometry and consequently high investment costs. This might not be an appropriate, cost-effective solution, so CREARE recommended multiple modules of smaller turbines. An alternative solution that can be easily realized is the radial turbine design concept.

There are two important reasons for adopting a radial-inflow concept. First, the specific mechanical energy of the stage is higher than that of the axial stage, which means a smaller-sized turbine is used. Second, because of the double-inlet configuration that can be used, the radial rotor is inherently stiff. These circumstances permit the blading to be fabricated from either thin, rolled sheet metal or cast plastic, which would reduce the investment cost considerably.

5.2 The Mixed-Flow Turbine Concept

The concept evaluated in this study is shown in Figure 5-1. Steam is introduced to the perimeter of a wheel from position 1. The inlet can be introduced at one point with a scrolled plenum to minimize pressure losses. As it enters the wheel, the flow divides into two sets of mirror-image flow passages formed by turbine blades that are shaped so as to absorb momentum from the flowing gas as it expands through the channels and changes direction from radially inward to axial in both of the axial directions, as shown. The axial flow is collected in a toroidal and probably scrolled exit diffuser at position 4 which collects the exhaust steam in circumferential flow and discharges it by radial outflow through an exit pipe at position 5.

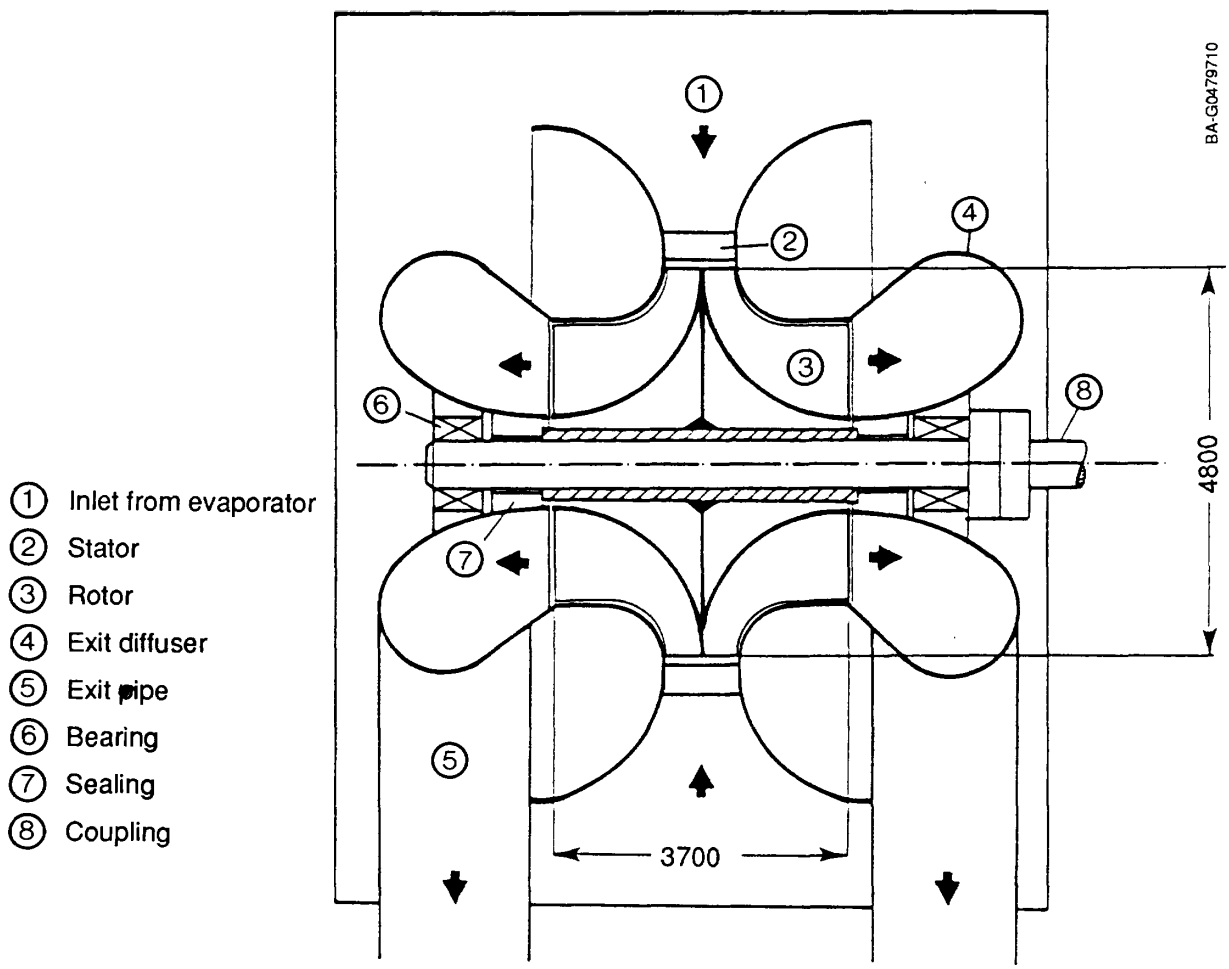

Figure 5-1. Single-stage, double-inflow radial steam turbine (dimensions are in mm)

The existing radial turbine design technology, unlike the radial turbine for open-cycle OTEC applications, deals with relatively high enthalpy differences and low mass flows. No information is yet available on the application of the radial turbine design to conditions like those of open-cycle OTEC. This gives rise to a need for investigating the problem systematically. In the following sections, the parameters defining the radial stage are derived. Then the radial cascade flow is investigated, in which the lift solidity ratio functions are derived. These relations, along with significant loss correlations, are then implemented into a design procedure for a systematic optimum design of radial-inflow turbines and their application to open-cycle OTEC conditions.

5.3 Performance Analysis

5.3.1 Description of Radial Stages

As Schobeiri shows [19], a turbomachinery stage can be described simply by the following stage parameters:

$$\mu_S = \frac{V_{m1}}{V_{m2}} , \quad \mu = \frac{V_{m2}}{V_{m3}} , \quad \nu = \frac{U_2}{U_3}$$

$$\phi = \frac{V_{m3}}{U_3} , \quad \lambda = \frac{l_m}{U_3{}^2} , \quad r = \frac{\Delta h_R}{\Delta h_R + \Delta h_S} ,$$

where mean steam velocity V_m and blade velocity U are taken from the velocity diagram (Figure 5-2), and Δh_R and Δh_S are the specific static enthalpy differences in rotor and stator. The dimensionless parameters μ_S and μ represent the meridional velocity ratio for the stator and rotor, respectively; ν is the circumferential velocity ratio; ϕ is the stage flow coefficient; λ is the stage load coefficient; and r is the degree of reaction. Introducing these parameters into the equations of continuity, moment of momentum, and the relation for degree of reaction, we can define the radial turbine stage completely by a set of four equations:

$$\cot\alpha_2 - \cot\beta_2 = \frac{\nu}{\mu\phi} \tag{5-1}$$

$$\cot\alpha_3 - \cot\beta_3 = \frac{1}{\phi} \tag{5-2}$$

$$\lambda = \phi(\mu\nu\cot\alpha_2 - \cot\beta_3) - 1 \tag{5-3}$$

$$r = 1 + \frac{\phi^2}{2\lambda} \{1 + \cot^2\alpha_3 - \mu^2 (1 + \cot^2\alpha_2)\} . \tag{5-4}$$

These equations can be expressed in terms of the flow angles α_2, α_3, β_2, and β_3, which lead to a set of four nonlinear equations:

$$\mu^2\phi^2(1-\nu^2)\cot^2\alpha_2 + 2\mu\nu\phi\lambda\cot\alpha_2 - \lambda^2 - 2(1-r)\lambda + (\mu^2-1)\phi^2 = 0 \tag{5-5}$$

$$\phi^2(1-\nu^2)\cot^2\alpha_3 + 2\phi\lambda\cot\alpha_3 + \lambda^2 - 2(1-r)\lambda\nu^2 + (\mu^2-1)\phi^2\nu^2 = 0 \tag{5-6}$$

$$(1-\nu^2)(\mu\phi\cot\beta_2+\nu)^2 + 2\nu\lambda(\phi\mu\cot\beta_2+\nu) - \lambda^2-2(1-r)\lambda + (\mu^2-1)\phi^2 = 0 \tag{5-7}$$

$$(1-\nu^2)(\phi\cot\beta_3+1)^2 + 2\lambda(\phi\cot\beta_3+1) + \lambda^2-2(1-r)\lambda\nu^2 + (\mu^2-1)\phi^2\nu^2 = 0 . \tag{5-8}$$

Equations (5-1) to (5-4) and (5-5) to (5-8), which reflect the conservation laws of thermo-fluid mechanics, include nine unknowns. The other five parameters required to solve these sets of equations can be defined from the boundary conditions pertaining to the problem under consideration. For a preliminary design, for example, the circumferential velocity or diameter ratio ν can be assumed as given. Furthermore, for a single-stage machine, the

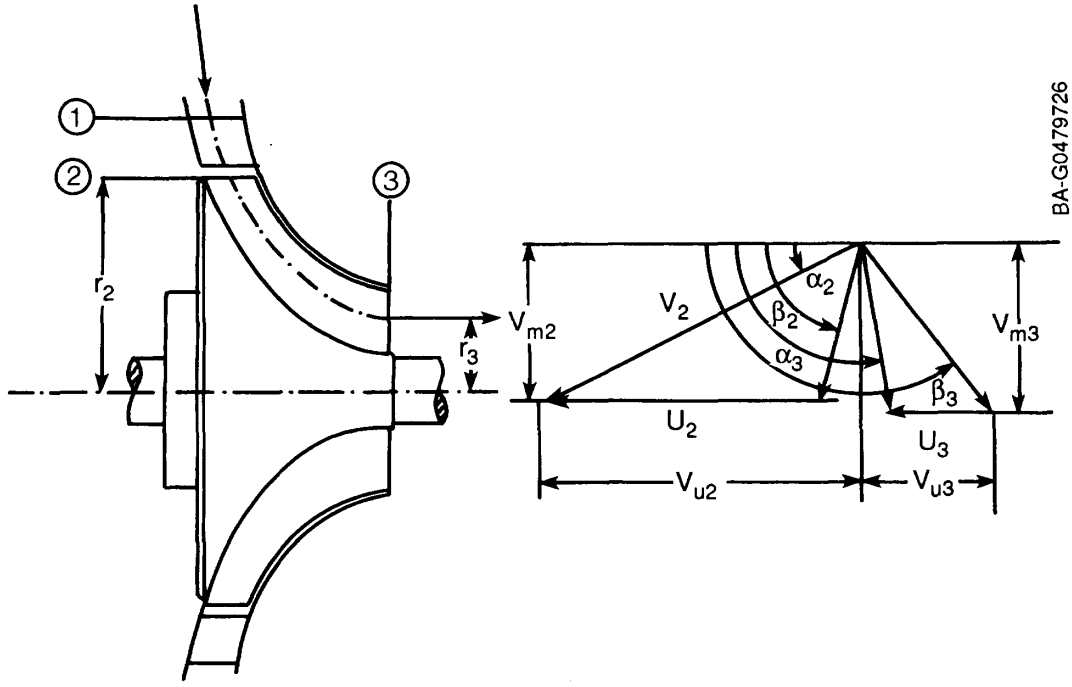

Figure 5-2. Radial-inflow turbine: velocity diagram, angle definition

absolute exit flow angle can be set at $\alpha_3 \approx 90°$, for a minimum exit loss. Additional information is provided if the enthalpy difference is known. This, in connection with the known network frequency and the outer diameter, determines the stage load coefficient λ. The stage flow coefficient ϕ can be estimated from the turbine mass flow $\hat{m}$ which dictates the turbine power. The meridional velocity ratio μ affects the type of blade. With Eqs. (5-1) to (5-4) or (5-5) to (5-8), the turbomachinery stage is described completely.

5.3.2 Radial Cascade Aerodynamics and Optimum Lift-Solidity Coefficient

Optimum design of the turbine component necessitates information about the optimum lift-solidity coefficient. The corresponding relationship derived by Zweifel [20] for the axial turbine is restricted to stage flows in which the stream lines are parallel to the cascade axis. Similar situations are encountered in high-pressure stages of an axial turbine or compressor, where the stream surfaces are approximated by cylindrical sections with constant diameters. In general, the flow through the intermediate- and low-pressure stages of axial machines, and also through the stages of radial machines, has stream surfaces with different radii that result in different blade spacing at the inlet and exit. Furthermore, the meridional velocity at the inlet might differ from that at the exit. The Zweifel criterion does not account for these differences. In order to calculate the blade lift-solidity coefficient correctly, the radius and the axial velocity changes must be taken into account. In the following, the corresponding relations for a turbine stator and rotor are derived. Extending the derivation to compressor stator and rotor leads to the same results.

Calculating the lift-solidity coefficient for a viscous flow requires the equations of continuity, momentum in circumferential and meridional directions, and the energy equation. As a result, a relation is obtained that contains the profile loss coefficient [19].

Because in calculating the optimum lift-solidity coefficient, the contribution of the profile loss coefficient is negligible, the flow can be considered inviscid. For an inviscid incompressible flow through the turbine stator shown in Figure 5-3, the lift force is given by the Kutta-Joukowski relation:

$$\vec{F}_i = \rho_\infty \vec{V}_\infty \times \vec{\Gamma} \ , \tag{5-9}$$

where the subscript i refers to the inviscid flow. The circulation is

$$\Gamma = \int_c \vec{V} \hat{} d\vec{c} = V_{u1} s_1 + V_{u2} s_2 + \int_2^3 \vec{V} \hat{} d\vec{c} + \int_4^1 \vec{V} \hat{} d\vec{c} \ . \tag{5-10}$$

Because the last two integrals cancel each other, Eq. (5-10) reduces to

$$\Gamma = V_{u1} s_1 + V_{u2} s_2 = s_2 \, (V_{u2} + V_{u1}) \ . \tag{5-11}$$

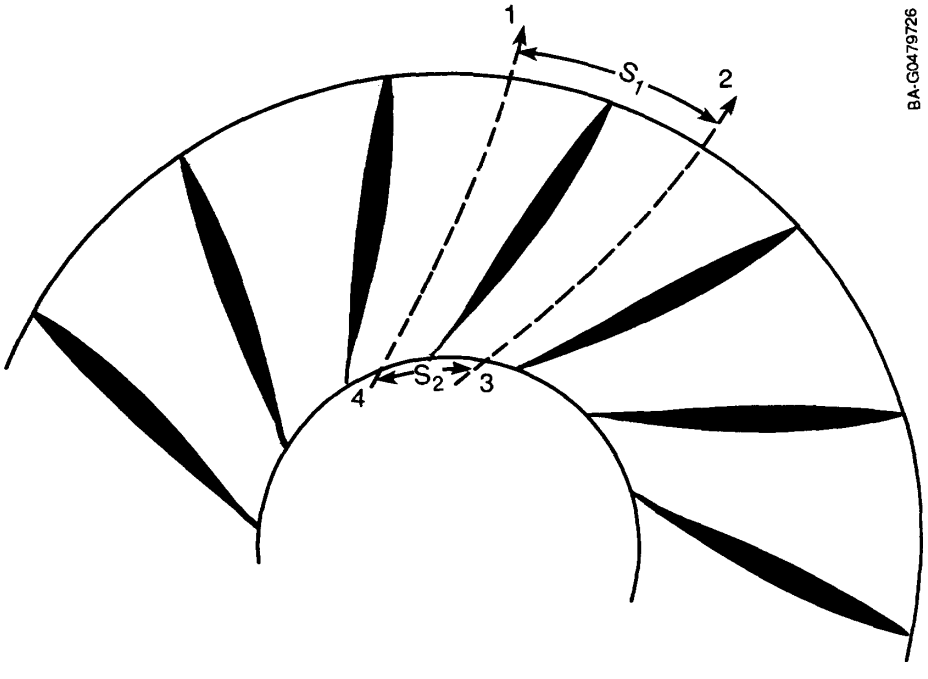

Figure 5-3. Circulation around a radial cascade

The magnitude of the mean velocity vector is

$$V_\infty = \frac{1}{2}\frac{V_{m2}\,(1 + \mu_S)}{\sin\alpha_\infty} , \tag{5-12}$$

where $\sin\alpha_\infty$ can be obtained from

$$\cot\alpha_\infty = \frac{\mu_S\cot\alpha_1 + \cot\alpha_2}{1 + \mu_S} . \tag{5-13}$$

Introducing Eqs. (5-11) and (5-12) into (5-9), we find that the stator lift coefficient for an inviscid flow is

$$C_L\frac{c}{s_2} = \frac{\sin^2\alpha_2}{\sin\alpha_\infty}(1 + \mu_S)[\cot\alpha_2 - \nu\mu_S\cot\alpha_1] . \tag{5-14}$$

Similarly, the lift solidity coefficient for a rotor in the relative frame of reference is obtained from

$$C_L\frac{c}{s_3} = \frac{\sin^2\beta_3}{\sin\beta_\infty}(1 + \mu)[\nu\mu\cot\beta_2 - \cot\beta_3] . \tag{5-15}$$

To calculate the rotor lift solidity coefficient in an absolute frame of reference, we must first calculate the absolute circulation. This and the dimensionless parameters defined above and the relations for the circumferential velocities yield

$$C_L\frac{c}{s_3} = \frac{\sin^2\alpha_3}{\sin\alpha_{\infty R}}\frac{(1 + \mu)}{\phi}[\mu\nu\phi\cot\beta_2 - \phi\cot\beta_3 + \nu^2 - 1] . \tag{5-16}$$

Equations (5-14) to (5-16) determine the lift-solidity coefficient for radial stator and turbine cascades. The optimum solidity and the number of the blades can be found if the optimum lift coefficient is known. Pfeil's systematic experimental investigations on a great number of stationary turbine cascades [21, 22] show that

$$(C_L)_{opt} \approx 1.0 .$$

The optimum solidities for stator and rotor are easily found by applying this criterion to Eqs. (5-14) and (5-15) or to Eq. (5-16) if the transformed $(C_L)_{opt}$ is known.

5.3.3 Calculation of Stage Efficiency

To calculate the stage efficiency, we must first identify the individual stage losses. The significant losses determining the efficiency of a double-inflow, single-stage, radial steam turbine are exit, primary (profile), and secondary losses. In the calculation procedure, however, the less significant losses such as trailing edge and wetness losses are also incorporated. In contrast

to what is known for the axial machine, we lack published data on systematic investigations of the radial turbine. However, it is reasonable to extend the correlations for an axial-flow turbine to radial machines.

5.3.4 Profile Losses

Turbine profile loss correlations, among others [23-27], generally consider the influence of flow deflection, solidity, Mach number, and Reynolds number. Triebnig et al. [28] discuss the possibility of optimum design. Pfeil's work [22] is the most recent comprehensive information on the optimum loss correlations for turbine cascades. From experimental investigations for turbine and compressor cascade profiles with the thickness-chord ratio (t/c) = 0.15-0.1, hydraulically smooth surfaces, and the Reynolds number

$$Re_{ref} = 3.5 \times 10^5 ,$$

Pfeil [25] proposes for optimum profile losses the correlation

$$\zeta = K_1 \left\{ 1 + K_2 \left(\frac{c}{s}\right)^3_{opt} \right\} C_L \frac{c}{s} \frac{1}{\sin\alpha_\infty} , \qquad (5\text{-}17)$$

where ζ is defined as the ratio of the total pressure difference divided by exit kinetic energy, with $K_1 = 0.0107$ and $K_2 = 0.25$ for axial machines.

For radial turbine applications, the incorporation of Eq. (5-17) into the efficiency calculation procedure with the constant $K_1 = 0.0215$ and the Reynolds number correction

$$\frac{\zeta}{\zeta_{ref}} = \left(\frac{Re_{ref}}{Re}\right)^{0.2}$$

yields reasonable results. The stage profile loss consists of the stator and the rotor total pressure losses that lead to the stage profile loss coefficient Z_p:

$$Z_p = \zeta_{ps} \frac{V_2^2/2}{l_m} + \zeta_{pr} \frac{W_3^2/2}{l_m} .$$

5.3.5 Secondary Losses

The principal concept of secondary flow loss calculations is based on the analogy between the drag forces induced by secondary flow within the cascade and the wing tip vortices generated by a wing with infinite length. For an elliptical lift distribution, Prandtl [29] found an analytical relation between the induced drag and the lift. Since then, we encounter that relation in many publications dealing with the calculation of secondary flow losses within the turbomachinery stages. Based on the results of Wolf [30], Utz [31], and Roeder [32], Traupel [24] developed a secondary flow loss correlation. Berg [33] investigated the influence of stage load parameter λ,

particularly on the secondary flow losses. The results of his investigations on five different axial turbine rotors without shrouds lead to the correlation used in this report:

$$\zeta_s = K\Lambda \left(\frac{\delta - \delta_o}{c}\right)^m , \tag{5-18}$$

where Λ is the lift function,

$$\Lambda = 4(\cot\beta_2 - \cot\beta_3)^2 \frac{\sin^2\beta_3}{\sin\beta_\infty} . \tag{5-19}$$

In Eq. (5-18), δ represents the actual tip clearance and δ_o the smallest tip clearance that does not cause a tip clearance flow. The constants $K = 0.169$, $m = 0.6$, and $\delta_o/c = 0.005$ were found from experiments. Applying this relation to the radial turbine stage yields

$$\zeta_s = 0.169(1 + \mu)^2(\nu\mu\cot\beta_2 - \cot\beta_3)^2 \frac{\sin^2\beta_3}{\sin\beta_\infty} \left[\frac{\delta - \delta_o}{c}\right]^{0.6} .$$

This correlation considers all significant parameters governing the radial stage secondary flow and is incorporated into the loss calculation procedure. The stage secondary flow loss coefficient is calculated from

$$Z_s = \zeta_{sS} \frac{V_2^2/2}{l_m} + \zeta_{sR} \frac{W_3^2/2}{l_m} .$$

5.3.6 Exit Losses

For a single-stage machine, the exit loss has a significant influence on the overall stage efficiency. The exit loss coefficient is defined as the ratio of the exit kinetic energy with respect to the specific mechanical energy of the stage l_m:

$$Z_e = \frac{V_3^2/2}{l_m} = \frac{V_3^2}{2\lambda U_3^2} . \tag{5-20}$$

Expressing the exit velocity vector V_3 in terms of the axial velocity component and using the stage dimensionless parameter, we can write Eq. (5-20) as

$$Z_e = \frac{\phi^2}{2\lambda(\sin\alpha_3)^2} . \tag{5-21}$$

5.3.7 Stage Loss Coefficient and Stage Efficiency

After calculating the individual stage loss coefficients Z_i, we can calculate the stage loss coefficient as

$$Z = \sum_{i=1}^{n} Z_i = Z_p + Z_s + Z_e + \ldots\ldots\ldots \tag{5-22}$$

where the index i represents the individual stage losses (for example, profile losses and secondary losses). The isentropic stage loss coefficient A_s is

$$Z_s = \frac{\Delta h_{loss}}{\Delta H_s} , \tag{5-23}$$

where Δh_{loss} represents all the enthalpy losses from the different loss mechanisms, and ΔH_s the available stage isentropic enthalpy difference. For the turbine stage, Eq. (5-23) is written as

$$Z_s = \frac{\Delta h_{loss}}{l_m + \Delta h_{loss}} = \frac{Z}{Z + 1} , \tag{5-24}$$

with the stage loss coefficient Z from Eq. (5-22).

The stage isentropic efficiency for the turbine stage is defined as the ratio of the actual total enthalpy difference, which is identical with the stage mechanical energy, divided by the isentropic stage total enthalpy difference. The isentropic stage efficiency in terms of Z_s is

$$\eta_s = \frac{\Delta H}{\Delta H_s} = \frac{l_m}{\Delta H_s} = \frac{\Delta H_s - \Delta h_{loss}}{\Delta H_s} = 1 - Z_s , \tag{5-25}$$

and in terms of Z is

$$\eta_s = \frac{\Delta H}{\Delta H_s} = \frac{l_m}{\Delta H_s} = \frac{l_m}{l_m + \Delta h_{loss}} = \frac{1}{1 + Z} . \tag{5-26}$$

5.4 Optimum Design of a 30-Hz Radial Steam Turbine with 2.8-MW Output

For open-cycle OTEC conditions, an optimum double-inflow radial steam turbine can be found. A calculation procedure is established that contains the relations derived above. To accurately calculate the turbine expansion line, we implement the standard steam properties program in the calculation procedure. To find the optimum solution, the significant parameters must be identified. This requires a systematic parameter study, from which the best combination of stage parameters with respect to optimum efficiency is selected. In the following sections, a single-stage and a two-stage turbine are investigated.

5.4.1 Single-Stage, Double-Inflow Radial Steam Turbine

Starting with a turbine frequency n = 30 Hz, an exit radius r_3 = 1.2 m, which is dictated by the turbine mass flow, and the exit blade height, we can investigate the influence of the stage parameters. Figure 5-4 shows the exit loss coefficient ζ_e versus the diameter ratio ν with α_2 as a parameter. Increasing ν decreases the exit loss. A large exit radius, however, results in a very large machine size, which is not desirable. In Figure 5-5, ζ_e is plotted against the stage flow coefficient ϕ with α_2 as a parameter. As expected, a higher stage flow coefficient ϕ that decreases with the radius ratio ν (Figure 5-6) results in higher exit losses ζ_e. Figure 5-7 shows the course of the degree of reaction r versus the diameter ratio ν. For the axial velocity ratio μ = 1, the inlet flow angle α_2 has no influence on the degree of reaction r. The stage isentropic efficiency η_s versus the flow coefficient ϕ with α_2 as a parameter is shown in Figure 5-8. The optimum efficiency decreases with increases in the inlet flow angle α_2. Detailed information about the efficiency and the geometry is given in Figures 5-9 and 5-10. The most significant parameter determining the efficiency and the geometry of the turbine stage are the diameter ratio ν and the inlet flow angle α_2. As shown in Figure 5-7, the maximum efficiency occurs at a relatively high diameter ratio ($\nu \simeq 2.0$) and low inlet flow angle ($\alpha_2 = 20$). A high diameter ratio causes an increase in the overall size of the machine, whereas a small inlet flow angle results in a very high exit blade height. Between these two opposite tendencies is an optimum solution with an acceptably high efficiency and size. As an acceptable compromise, a reasonably good efficiency η_s = 82.18% is obtained for ν = 1.8 and $\alpha_2 = 35°$ (Figure 5-9). The corresponding turbine configuration is shown in Figure 5-1.

5.4.2 Mechanical Design

No mechanical design effort has been applied to the design of a radial-inflow machine except to define the overall turbine wheel dimensions, as shown in Figures 5-1 and 5-11. The single- and two-stage options presented by the Texas A&M team point out the opportunity for a design trade-off between the turbine wheel diameter and the overall turbine length. The two turbine designs described operate at 1800 rpm and deliver 2.8 MW to a generator input. The preferred approach can be selected based on the definition of the enclosure design (not yet defined). The preliminary layout of the alternate concepts suggests that the enclosure can very easily reach a size approximately 7-8 m in diameter and 8.5-9.5 m long. Thus, the design and cost of this enclosure will become the primary cost drivers in the concept.

The advantage of the mixed-flow rotor configuration is that the structural and dynamic characteristics of the wheel can be projected and achieved with the least risk of any of the options studied. A radial line configuration that can be defined for mixed-flow blading will put all elements of the blading into tension, primarily arising from centrifugal forces. We expect that the blading, shaft, and bearings can be designed using a relatively lightweight, conservative design.

5.4.3 Two-Stage, Dual-Inflow Radial Steam Turbine

A simple, economical solution that can reduce the size and increase the output of the turbine is the multistage configuration. In this case, identical

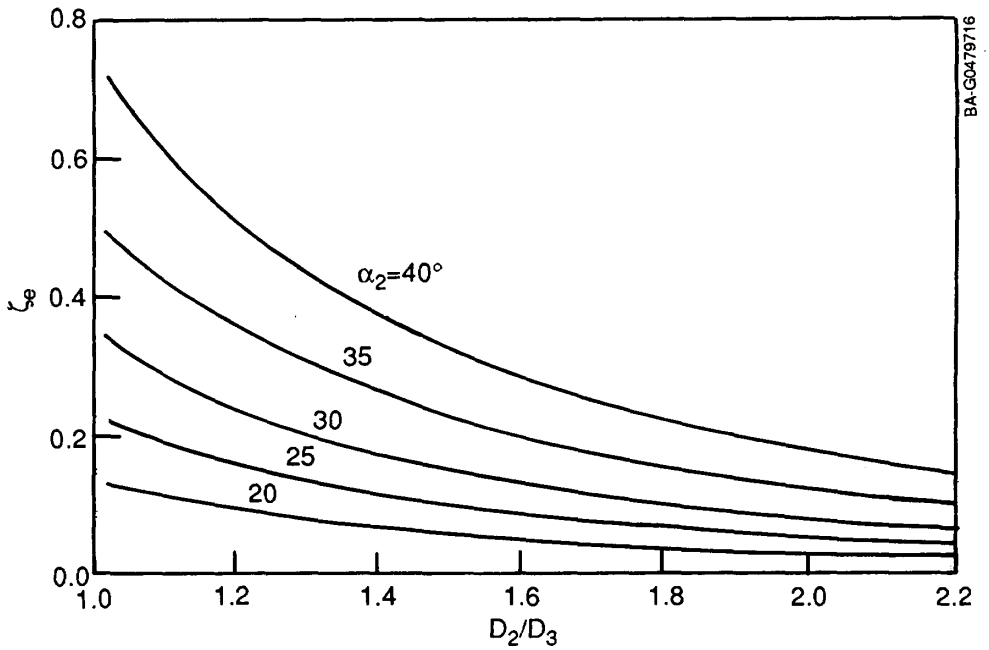

Figure 5-4. Exit loss coefficient ζ_e as a function of diameter ratio $\nu = D_2/D_3$, with the absolute inlet flow angle α_2 as a parameter

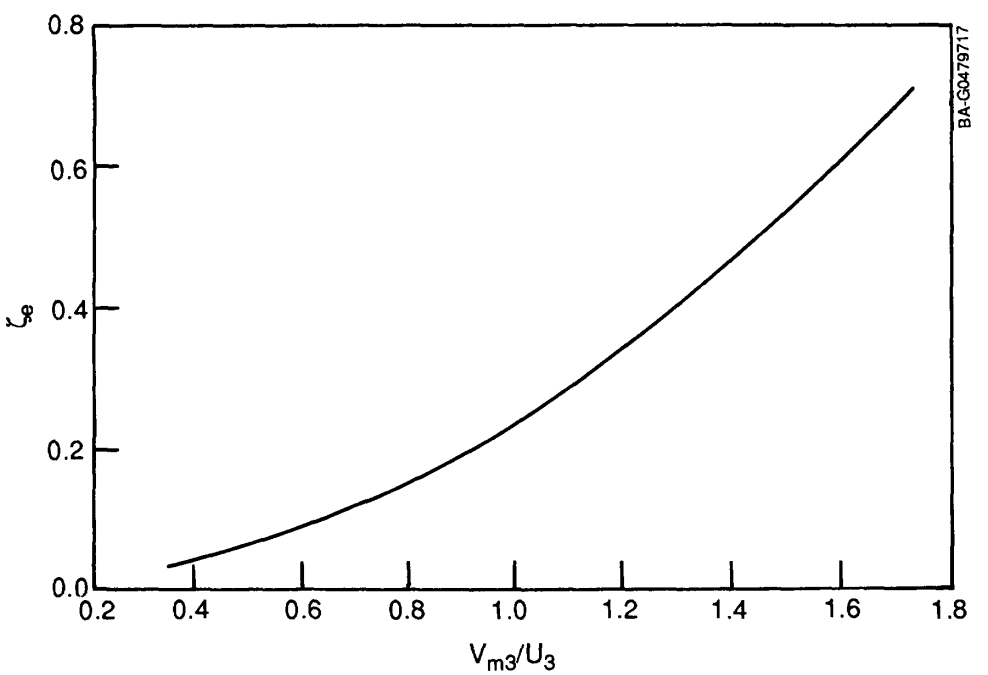

Figure 5-5. Exit loss coefficient ζ_e as a function of flow coefficient $\phi = V_{m3}/U_3$, with the absolute inlet flow angle α_2 as a parameter

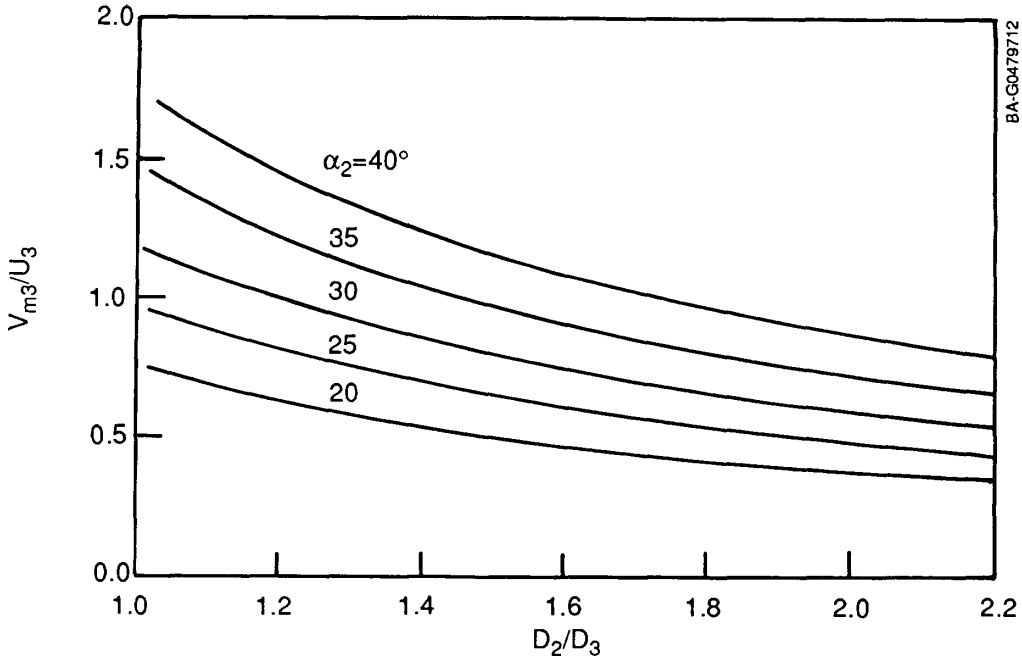

Figure 5-6. Stage flow coefficient $\phi = V_{m3}/U_3$ as a function of diameter ratio $\nu = D_2/D_3$, with the absolute inlet flow angle α_2 as a parameter

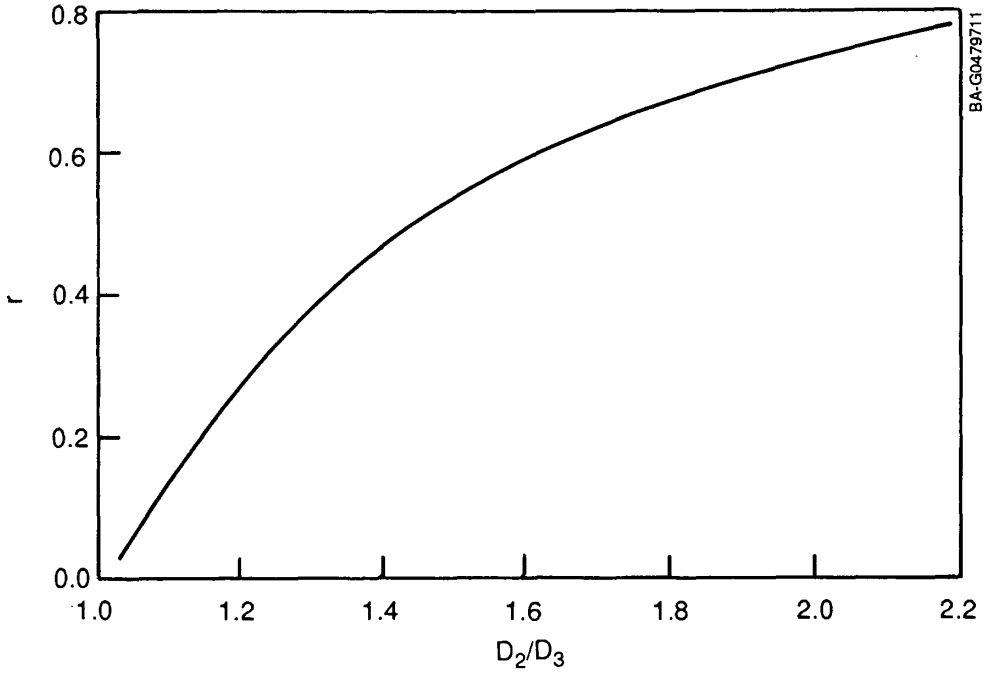

Figure 5-7. Degree of reaction r as a function of diameter ratio $\nu = D_2/D_3$, with the absolute inlet flow angle α_2 as a parameter

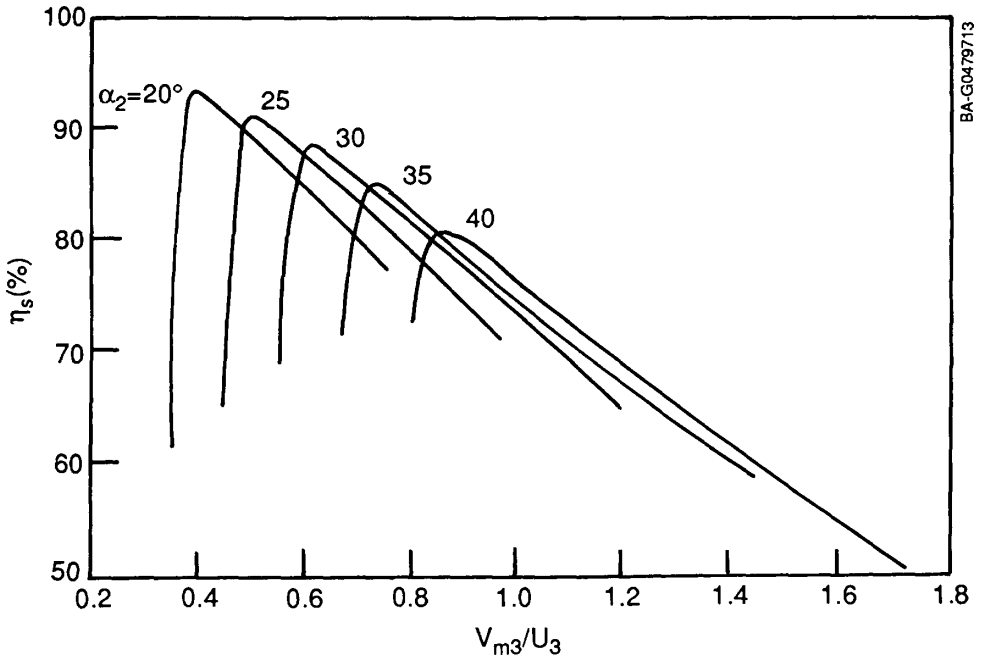

Figure 5-8. Stage isentropic efficiency η_s as a function of stage flow coefficient $\phi = V_{m3}/U_3$, with the absolute inlet flow angle α_2 as a parameter

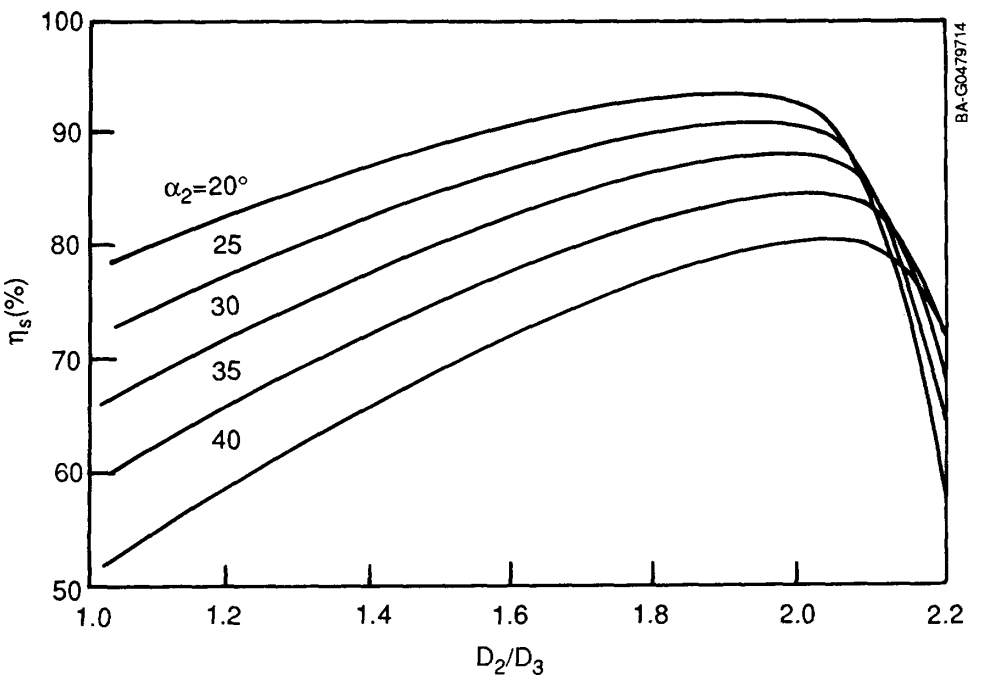

Figure 5-9. Stage isentropic efficiency η_s as a function of diameter ratio $\nu = D_2/D_3$, with the absolute inlet flow angle α_2 as a parameter, for the single-stage, double-inflow turbine

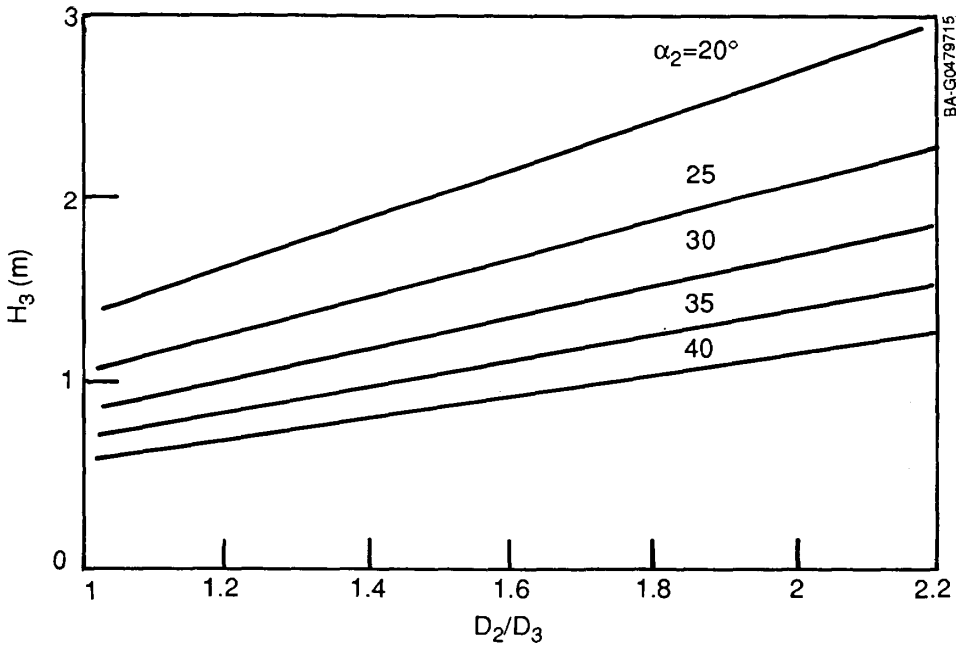

Figure 5-10. Exit blade height H_3 as a function of stage diameter ratio $\nu = D_2/D_3$, with the absolute inlet flow angle α_2 as a parameter

stages can be used that are designed for the same inlet and exit conditions. Figure 5-11 shows a two-stage configuration with two separate inlets and exits. As shown in Figure 5-12, for an exit radius r_3 = 1 m, ν = 2, and α_3 = 30°, a reasonably high efficiency (η_2 = 84.7%) could be achieved. The number of stages could be extended to that required to achieve plant capacity with the added complexity of inlet and outlet flow manifolding.

5.5 Conclusions and Recommendations

We have described a thermo-fluid design concept for a low-pressure, radial-inflow steam turbine for open-cycle OTEC. For optimum design, the necessary theoretical tools were developed and applied to a single- and a two-stage, double-inflow, radial steam turbine. For a single-stage turbine with output P = 2.8 MW, n = 30 Hz, μ = 1, ν = 1.8, r_3 = 1.2 m, and α_2 = 35°, an isentropic stage efficiency (η_s = 82.1%) was calculated. The design concept augments the turbine power by means of the dual-flow or multistage configuration. For a turbine with the same output and frequency as the single-stage turbine, with μ = 1, ν = 2.0, r_3 = 1.0 m, and α_2 = 30°, a reasonably high isentropic efficiency (η_s = 84.7%) was achieved. Mechanical design of the components, especially of the turbine enclosure, is required before any additional assessment can be made of the potential of this system concept to reach the performance and cost goals established by the project.

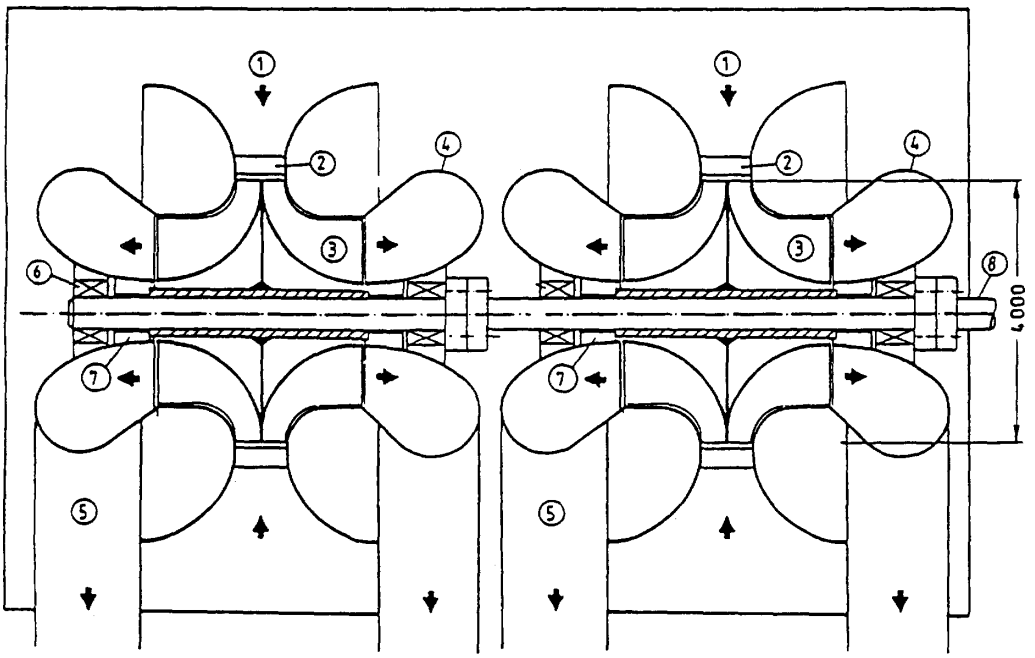

Figure 5-11. Two-stage, double-inflow radial steam turbine (dimensions are in mm). 1 = inlet from evaporator, 2 = stator, 3 = rotor, 4 = exit diffuser, 5 = exit pipe, 6 = bearing, 7 = sealing, 8 = coupling.

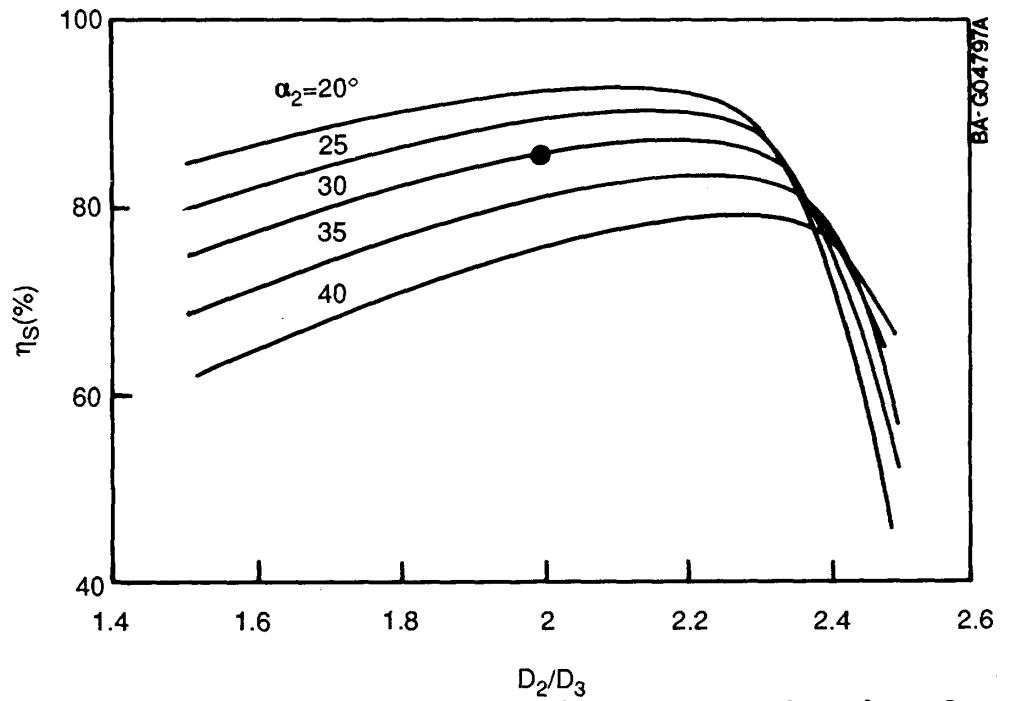

Figure 5-12. Stage isentropic efficiency η_s as a function of stage diameter ratio $\nu = D_2/D_3$, with the absolute inlet flow angle α_2 as a parameter, for the two-stage, dual-inflow turbine

5.6 System Cost

No cost projections were made on the mixed-flow configuration option. However, its primary cost advantage will probably lie in the fact that this option should take the least amount of time and cost the least to develop. No more definitive statements about costs can be made until preliminary mechanical design specifications are established.

6.0 SUMMARY AND DISCUSSIONS

6.1 Summary

Turbine costs represent a significant fraction of the total cost of an open-cycle OTEC system. The high specific volume, low temperature, and low pressure ratio of the working fluid expanding through an OTEC turbine provide researchers with opportunities to examine new materials and design options for the construction of such turbines.

Turbines are classified into radial-, axial-, and mixed-flow machines. Choosing which type to use depends on the application, and the best choice is not always clear-cut. However, in comparing turbines of the same diameter, we can state that the axial configuration is capable of handling much higher flow than the other configuration options. On the other hand, at lower flow rates, a radial machine can have a higher energy conversion efficiency. The radial turbine stage is capable of operating at a higher pressure ratio than an axial stage. However, staging of axial turbines is much easier to arrange and a large turbine pressure ratio is easy to achieve with axial turbines. For these reasons, and because the primary energy sources in the world's economy produce high steam flow rates at high pressure ratios, multistage axial-flow turbines oriented on a horizontal axis have accounted for virtually all of the rotating energy conversion equipment in use today. The major exceptions are the mixed-flow, vertical-axis turbines used in many hydroelectric installations, the mixed-flow turbines used in vehicular turbochargers, and the high-performance, multistage radial-flow steam turbine system developed by the Jungstrom Turbine Company.

One result of this focus on axial designs is a highly developed fluid dynamics, structural, and materials technology base. This data base has allowed us to take these designs to the limits of their capability in terms of efficiency and structural integrity. Low-pressure stages of a steam turbine are highly twisted to accommodate the radial variations in blade speed inherent in the long blades needed at low pressures. These long blades are carefully designed to avoid structural failure due to premature metal fatigue, with particular emphasis on the dynamic response of the blades. Choices of materials are also driven by erosion and corrosion considerations caused by the steam condensate present at the turbine's exhaust. Thus, LP turbine blades tend to have a complex shape, be massive in size (for stiffness), and utilize high-strength alloys (like titanium). The industry makes blades up to 1.32 m (52 in.) long, and it is not likely that larger ones will be available if the currently available technology is used.

Within the context of this available technology, it was appropriate to examine turbine options that represent some major departures from the state of the art. Since detailed design and cost estimates do not exist for a baseline turbine-generator design employing current stator and rotor hardware, a rough order-of-magnitude estimate was established by expert consultants as a point of reference for all the comparisons. The consultants estimated that such a system would cost approximately $3.4 million, with an estimated power output of 1.2 MW. The turbine system cost, $2833/kW, far exceeds the technology cost goals ($1000/kW) established in system feasibility studies.

The results in this study represent a revolutionary rather than evolutionary approach to the turbine problem. The three concepts studied reflect the three major flow-path geometry classifications usually considered in turbine design. But the studies went beyond flow geometry and considered new materials and an innovative approach for integrating the turbine into the balance of the system hardware as ways of reducing system costs. The three innovative approaches to open-cycle OTEC turbine design and construction were defined and evaluated in a preliminary way.

The first approach calls for a crossflow configuration. This innovative design makes use of simple, two-dimensional blading that can be fabricated of inexpensive materials or high-strength composite plastics. A particular innovation in this design is a floating stator design that promotes more ideal flow into the second-stage expander. Scale up of this concept is the simplest of all the concepts examined, because all that is required is a simple extension of the blade length. The form factor of the inlet and exhaust gas plenums permits compact, efficient interfaces with the system's heat exchangers. The projected efficiency of the crossflow configuration is the lowest of the options examined, however. Because it is a two-stage turbine, the blade tip speed at optimum efficiency is the lowest of the options. Clearly, the crossflow turbine technology is the least developed of the options; commercial hardware is restricted to the hydraulic turbine system and several air compressor systems designed for specialized applications.

Second, a design and performance analysis of an axial-flow turbine operating in a vertical-axis orientation shows that using composite plastic blading, we can construct a lightweight rotor with accompanying lightweight bearings and mounting pedestal. The vertical orientation, facilitated by the lightweight composite turbine wheel construction, permits efficient vacuum enclosure of the turbine and the heat transfer subsystems. Both aspects contribute to cost reductions and ought to be pursued with equal vigor.

Third, a multiple mixed-inflow configuration was defined that may result in the highest system efficiency of any concept studied. Employing radial inline construction, the inherently stiff, structurally rugged mixed-flow blades are good candidates for low-cost blade construction. The dual-flow configuration can be used in parallel with multiple wheels on a common shaft so that scale up can be achieved incrementally without the need to develop new blading and a new turbine wheel.

Each of the turbine concepts is described at a conceptual design level. Performance is described by using widely different mathematical models. The axial machine is described by its similarity to a carefully analyzed, larger-scale turbine. The performance of the mixed-flow design is described by using a two-dimensional flow field and well-documented loss correlations. The crossflow system is analyzed by using a one-dimensional flow field and the Soderburg relationships to describe losses.

Attempts have been made to estimate costs for the axial and crossflow configurations. These should be considered as rough indicators, at best. No attempt was made to characterize the cost of the mixed-flow configuration.

The following section contains a discussion of four aspects of the cost-reduction problem. We explore the economic merit of increasing the turbine's

output by increasing mass throughput in excess of that indicated for maximum efficiency. The discussion is probably applicable to all three turbine flow classifications in varying degrees. We also explore the pros and cons of the three flow options and provide some concluding remarks on the results obtained in this study.

6.2 Discussion of Results

This study shows that there are a number of ways to improve the cost effectiveness of the energy-conversion portion of an open-cycle OTEC system. The system that is ultimately found to be economically viable will be developed based on some combination of these improvements. These approaches to cost reductions can be divided into three areas:

- Definition of the rotor design and operating parameters for maximum power output
- Design of a rotor configuration and materials for minimum cost consistent with performance and durability requirements
- Reduction of the cost of the turbine enclosure through simplification or integration with system containment, or both.

The results of the studies are discussed in the context of these three areas of approach.

6.2.1 Rotor Design and Operating Parameters for Maximum System Power Output

MIT's study found that the design and operating parameters needed for maximum efficiency of a turbine rotor are not necessarily associated with the most economical system design. These conclusions, presented in Section 2.0, apply to an axial-flow design and are based on certain assumptions about the cost breakdown among the major system components and the sensitivity of those components to the size of the system. The assumptions appear to be a valid starting point, but the numbers must be refined by a more detailed system analysis to validate the conclusions. An interesting extension to Table 2-3 would be to incorporate the results reported by CREARE on turbines using existing blading into the table as well as the University of Pennsylvania projections on a wheel using composite plastic blading. Table 6-1 summarizes these results and shows that developing an advanced rotor has the potential to double the power output of an open-cycle OTEC power module and to reduce the installed turbine/generator capital cost by 65%. Simply going from a high-efficiency to a high-power design has a 15% impact on the system cost.

The results summarized in Table 6-1 lay out a turbine development path for the open-cycle OTEC program. The first two options show that existing hardware can be used to conduct proof-of-concept experiments or to construct special-situation OTEC plants. The turbine design based on 1.32-m (52-in.)-long blades is within the realm of existing technology but requires substantial redesign and retooling for commercialization. If new blade materials can be developed and verified experimentally, the OTEC community could move closer to program cost goals. The table does not show data for yet another significant step in approaching these goals that could be even more economically beneficial, which involves using simple, two-dimensional blades assembled in a cantilever configuration.

Table 6-1. Costs of Open-Cycle OTEC Systems Using Conventional and Innovative Turbine Concepts

Turbine/Generator		Efficiency	Cost	Turbine Cost	
Type[a]	Power	(%)	($M)	($/kW)	Status
(1)	1.2 MW	64	$3.4	$2833	Existing hardware
(2)	1.4 MW	74	$3.5	$2500	Mod. exist. hardware
(3)	1.74 MW	77	$3.5	$2010	New design
(4)	2.0 MW	74	$3.6	$1800	New design
(5)	2.39 MW	64	$3.7	$1548	New design
(6)	2.39 MW	64	$2.4	$1000	New technology

[a](1) Existing rotor and stator (L-1 stage); (2) existing rotor, new stator (L-1 stage); (3) new rotor and stator (high efficiency, LP stage); (4) new rotor and stator (baseline, LP stage); (5) new rotor and stator (high power, LP stage); and (6) advanced rotor and stator (high power, LP stage).

6.2.2 Innovative Rotor Configurations and Materials

The main thrust of this study was to identify and evaluate turbine rotor blading configurations and materials that could be incorporated into turbine designs and would cost significantly less to build than currently available hardware. Concepts reflecting the three primary blade types used in the industry were suggested and evaluated. In terms of thermodynamic performance, nothing unexpected was uncovered. There may be some profile blade loss effects as a result of the low Reynolds number for the flow passing through the turbine. Inlet and outlet hood losses would probably represent a larger fraction of the gross power produced than that of conventional systems. None of the concepts investigated incorporated a diffuser to recover a part of the energy in the turbine exhaust, which could be a significant amount of energy if the high-power approach to turbine design and operation is adopted. In all cases, the basis for optimistic cost projections revolves around the conclusion that using inexpensive, lightweight blading materials would reduce the cost and weight of the turbine wheel, and that, in turn, would reduce the weight and cost of the surrounding supporting structural members.

This is a powerful argument, especially because the weights and sizes of existing turbine technology are so large. For instance, the University of Pennsylvania projected that foam core blades could weigh 1/25 of their steel equivalents. This weight savings passes through to the turbine disk, because its primary function is to support the centrifugal load imposed by the rotating blades. The shaft, in turn, must be strong and stiff enough to support the total wheel mass and not allow a resonant response in the wheel at the frequencies associated with turbine rotation. Even if the turbine wheel design realizes only a fraction of the weight savings associated with new blade material, the impact on the mass of the rotor's supporting structure and on the bearing losses would be significant. It is worth noting that the bearing losses are not included in the analyses described in Table 6-1, but they are estimated to be in the range of 50-100 kW for the steel rotors

(Types 1-5) and 15-20 kW for the composite rotor. Incorporating these losses into the analysis would further enhance the benefits of developing the advanced rotor.

On the other hand, the structural and dynamic integrity of a composite turbine wheel over its operating life must be considered. Problems in defining the structural properties of such a structure, and then analyzing structural response, are evident in the difficulty that the Pennsylvania team encountered with the ANSYS model for a stress and vibration analysis. It will be important to achieve a high degree of stiffness in a composite structure in order to move the modes of blade vibration away from the turbine's rotational frequencies. Further concerns are related to the complex stresses set up within an axial blade because of twisting, bending, tension, and various combinations of all these forces.

The response of the laminate materials and interfaces to these forces and the effects of moisture and aging on the materials would have to be determined. The use of these materials in aircraft, aerospace, and automobiles has created a growing base of technical data to support further research and development. The cantilevered blade represents a step away from the potential problems of the axial blade design. MIT showed that, because the blades are two-dimensional rather than three-dimensional, they are much simpler to fabricate and could be made of simpler composites. In addition, the stresses imposed on a cantilevered blade are primarily associated with bending, so structural and dynamic designs can be approached with more confidence. A cantilevered blade turbine rotor should require less development time and a smaller investment than an equivalent axial design. However, the design of the cantilever blade wheel involves some technical uncertainty, and the crossflow approach entails the lowest efficiency and the least amount of design data available to the designer.

The Texas A&M team showed that the radial-inflow turbine represents a design that can be pursued with confidence. The thermodynamic design and performance are well characterized, and there is extensive correlation between theory and practice. Although there is not a lot of detail on the mechanical design of the rotor proposed in this report, similar configurations have been built using a radial line design that puts all of the blade elements in tension; the centrifugal forces act to keep the blade in its designed shape. A mixed-flow blade has a large ratio of blade length to diameter, and when this is combined with a double-inlet configuration, an inherently stiff rotor results. Scaling of the turbine-generator output is achieved by parallel multiple rotors on the power plant shaft. This approach keeps the enclosure diameter small (around 7-8 m) but requires multiple parallel rotors for larger plant capacities, such as 10 MW.

The difficulties that may be encountered with this concept are the complexity and potential flow losses associated with the supply and exhaust hoods. The research team that examined cantilevered options rejected radial inflow and outflow alternatives for this reason. Since neither that team nor the team that studied the mixed-flow design generated a design for the enclosure, supply hoods, and exhaust hoods, it is not possible to say with certainty how significant a factor that might be. However, in most open-cycle OTEC system designs prepared to date, the weight of the enclosure makes up a significant portion of the system's total weight, sometimes accounting for as much as

three-fourths of the total. For this reason, several innovative turbine design teams examined careful integration of the turbine with the balance of the system as a promising approach to cost reduction.

6.2.3 Integration of Turbine with System Enclosure

Each of the three studies made reference to the turbine enclosure as an important factor in a system cost-reduction strategy. There are two aspects to examine in regard to the enclosure design: its cost and its impact on fluid-dynamics losses in the turbine hoods. The enclosure is comparable to the rotor as a major cost contributor in a conventional turbine-generator. The size of an open-cycle OTEC turbine and the vacuum operating requirement make the enclosure cost an even larger fraction of the total cost in these systems. If innovations can bring down the cost of the rotor, the enclosure will be the primary driver of system cost. Several approaches to reducing the cost of the enclosure have been offered. In the case of a vertical-axis machine, it is possible to conceive a plant design in which the evaporator and condenser are axisymmetric with the turbine's axis. This concept could permit vacuum containment at the plant level, substantially reducing structural requirements for the internal turbine and heat exchanger shrouding required to direct the fluid flow. Another approach calls for reducing the size of the turbine wheel and achieving plant capacity by using multiple wheels on a common shaft. A smaller wheel size reduces the enclosure diameter needed but increases the enclosure length, which is more material-efficient.

Yet another approach attacks the performance aspect of the problem - the impact of the enclosure design (specifically, the hoods) on the turbine's efficiency. The crossflow design was selected in part because of its simple, straight flow paths for the steam, inlet, and exhaust. The axisymmetric, vertical-axis design eliminates turns of the steam at the low-pressure exhaust. While little or no mention was made of exhaust diffusers, they need to be considered, especially if a high-power design is adopted. Enclosing such a diffuser represents a major technical and cost issue in some of the turbine concepts.

6.3 Concluding Remarks

This study was directed at identifying operating and construction concepts that could significantly reduce the cost of an open-cycle OTEC turbine. This objective was met by evaluating the fluid-dynamics elements already developed along with new machine geometries and materials.

A key finding is that new rotor materials with high stiffness and strength-to-weight ratios can reduce the weight and cost of the turbine rotor and supporting structure. Some durability questions might be raised in regard to these materials. However, we have a substantial data base on related structures, such as windmills, helicopter blades, and airplane propellers, to draw from in developing such blading. A second finding is that the best choice among the axial, radial, or mixed-flow configurations is still in question. Axial designs have received the most attention over the last 20-30 years because they are easy to stage up to whatever number is required for a particular application. Since the pressure ratio in an OTEC application could be satisfied with a single stage of almost any geometry, a staging criterion should not be relevant; each of the options should be examined based on the cost of

the turbine wheel and supporting structure as well as the degree to which the flow geometry is integrated with the steam path from the evaporator to the condenser.

Some important additional information is needed before we can select an innovative turbine option and adequately assess its potential for cost-effective integration into a power system. Specifically, decision makers would be helped by these analyses:

1. A conceptual design and analysis of the turbine's performance and how it interfaces with the rest of the system. This should include a definition of all fluid-dynamics losses in the system, physical structure requirements to satisfy the containment and dynamics aspects of the design, and the cost of meeting performance and structural specifications.
2. An experimental evaluation of the physical properties and durability of candidate composite plastic materials that are considered for turbine rotors.

It appears feasible that an eventual turbine-generator cost approaching $1000/kW can be achieved for open-cycle OTEC applications.

7.0 ACKNOWLEDGMENTS

This report reflects the work of three university teams that completed their studies as a part of the work of their respective departments. Timothy Brehm, advised and directed by Prof. A. Douglas Carmichael of MIT's Department of Ocean Engineering, completed the work on the baseline definition and the cantilevered blading concepts. Paul Berman, Angelito Lucena, Tanya Moore, Chris Richardson, and Kevin Tzou completed the work on the vertical-axis, axial-flow turbine in the Mechanical Engineering Department of the University of Pennsylvania under the guidance of Dr. Noam Lior and with the assistance of several professors. The work on the double-inflow, radial steam turbine was completed and reported by Dr. Taher Schobeiri of the Department of Mechanical Engineering, Texas A&M University, assisted by Patrick Sparkman. The work done by these teams is gratefully acknowledged. In addition, important contributions to the report were made by SERI turbine consultants William Saunders, William Steltz, and Neville Reiger. Instructive comments and discussions by Desikan Bharathan and Andrew Trenka helped to bring some focus to these diverse research activities.

8.0 REFERENCES

1. Cohen, R., "Electric Power Generator--Ocean Thermal Energy Conversion," Chapter 13, Solar Energy Technology Handbook, New York: Marcel Dekker, Inc., 1980.

2. Cohen, R., "Energy from the Ocean," Phil. Trans. R. Soc. Land, A 307, 1982, pp. 405-437.

3. Penney, T., D. Bharathan, J. Althof, and B. Parsons, "Open-Cycle Ocean Thermal Energy Conversion (OTEC) Research: Progress Summary and Design Study," ASME Paper 84-WA/SOL-26 presented at the ASME Winter Meeting, New Orleans, LA, Dec. 9-14, 1984.

4. Block, D., and J. Valenzuela, Thermoeconomic Optimization of OC-OTEC Electricity and Water Production Plant, A Subcontract Report, SERI/STR-251-2603, Golden, CO: Solar Energy Research Institute, May 1985.

5. Westinghouse Electric Corporation, 100 MW OTEC Alternate Power Systems, Final Report, Contract No. EG-77-C-05-1473, U.S. Department of Energy, 1979.

6. CREARE, Inc., Design and Cost Study of Critical OC-OTEC Plant Components, Final Report, SERI/STR-252-3246, Golden, CO: Solar Energy Research Institute, June 1988.

7. Federal Ocean Energy Technology Plan: Multi-Year Program Plan, FY 85-89, U.S. Department of Energy, DOE/CH10093-100, Washington, DC: US DOE, December 1985.

8. Harms, V. W., and A. T. Dengler, "Seawater-Discharge Analysis and Effluent-Plume Characteristics for the STF-Upgrade Project (Keahole Point, Hawaii)," Marine Sciences Group-University of California, MSG-85-020, May 1985.

9. Coleman, W. H., J. D. Rogers, D. F. Thompson, and M. I. Young, "Open Cycle OTEC Turbine Design," AIAA Paper No. 82-2595, presented at the AIAA Second Terrestrial Systems Conference, Colorado Springs, CO, December 1981.

10. Thompson, D. F., K. A. McAfee, and M. I. Young, Advanced Ratio Design, OC-OTEC Turbine Rotor Structural Design Study, 1984 (unpublished).

11. Balje, O. E., Turbomachines: A Guide to Design, Selection, and Theory, New York: John Wiley and Sons, 1981.

12. CREARE, Inc., FLUENT User's Manual, Version 2.81, Telex Publishing, Hanover, NH, 1985.

13. DeSalvo, G. J., and J. A. Swanson, ANSYS Engineering Analysis System User's Manual, Swanson Analysis Systems, Inc., 1985.

14. Welsh, R. J., Plain Bearing Design Handbook, Thetford, England: Thetford Press, Ltd.

15. Bosser, E. R., and D. F. Wilcock, Bearing Design and Application, New York: McGraw Hill Book Co., 1957.

16. Mechanical Components Handbook, Parmley, R. O., ed., New York: McGraw Hill Book Co., 1985.

17. Parker, E. R., Materials Data Book for Engineers and Scientists, New York: McGraw Hill Book Co., 1967.

18. Christensen, K. M., Mechanics of Composite Materials, New York: John Wiley & Sons, 1979.

19. Schobeiri, T., "Lecture Notes on Turbomachinery," Graduate Course, Texas A&M University, Spring 1988.

20. Zweifel, O., "Die Frage der optimalen Schaufelteilung bei Beschaufelungen von Turbomaschinen insbesondere bei grosser Umlenkung in den Schaufelreihen," BBC-Mitteilung, Dez. 1945.

21. Pfeil, H., "Beitrag zur optimalen Auslegung von Axial-Schaufelgittern," Dissertation Darmstadt, D17, 1964.

22. Pfeil, H., "Optimale Primärverluste in Axialgittern und Axialstufen von Strömungsmaschinen," VDI-Forschuingsheft 535, 1969.

23. Ainley, D. G., and G. C. R. Mattieson, "An Examination of Flow and Pressure Losses in Blade Rows of Axial Flow Turbines," ARC-R&M, 1955.

24. Traupel, W., "Thermische Turbomaschinen," Bd. I, Springer Verlag, 1978.

25. Balje, O. E., and R. L. Binsley, "Axial Turbine Performance Evaluation Part A: Loss-Geometry Relationship," ASME Transactions, Series A, J. Eng. for Power, Vol. 90, October 1968.

26. Deic, T., "Untersuchung und Berechnung axialer Turbinenstufen," VEB Verlag Technik, Berlin, 1973.

27. Craig, H. R. M., and H. J. A. Cox, "Performance Estimation of Axial Flow Turbines," Proc. Inst. Mech. Engrs., 1970-71, Vol. 185, 32/71.

28. Triebnig, H., and D. K. Mukherjee, "Uber Verluste in Axialturbinenstufen und die Möglichkeiten einer optimalen Auslegung," VDI Zeitschrift, reihe 6, nr. 7, 1966.

29. Prandtl, L., and O. G. Tietjens, Applied Hydro- and Aeromechanics, New York: Dover Publications, Inc., 1934.

30. Wolf, H., "Die Randverluste in geraden Schaufelgittern," Wissenschaftliche Zeitschrift der Technischen Hochschule Dresden, 10, 1961, heft 2.

31. Utz, C., "Experimentelle Untersuchungen der Strömungsverluste in einer Mehrstufigen Axialturbine," Mitteilung des Institutes für Thermische Turbomaschinen der Eidgenissischen Technischen Hochschule Zürich, Nr. 19, 1972.

32. Roeder, A., "Experimentelle bestimmung der Einzelverluste in einer einstufigen Versuchsturbine," Mitteilung des Institutes für Thermische Turbomaschinen der Eidgenissischen Technischen Hochschule Zürich, Nr. 15, 1969.

33. Berg, H., "Untersuchunger über den Einfluss der Leistungszahl auf Verluste in Axialturbinen," Dissertation der Technischen Hochschule Darmstadt, D17, 1973.

Document Control Page	1. SERI Report No. SERI/TR-253-3549	2. NTIS Accession No.	3. Recipient's Accession No.

4. Title and Subtitle

Innovative Turbine Concepts for Open-Cycle OTEC

5. Publication Date
December 1989

6.

7. Author(s) Massachusetts Institute of Technology, Texas A&M University, University of Pennsylvania

8. Performing Organization Rept. No.

9. Performing Organization Name and Address
Massachusetts Institute of Technology
Cambridge, Massachusetts
Texas A&M University
College Station, Texas
University of Pennsylvania
Philadelphia, Pennsylvania

10. Project/Task/Work Unit No.
0E912032

11. Contract (C) or Grant (G) No.
(C)
(G)

12. Sponsoring Organization Name and Address

Solar Energy Research Institute
1617 Cole Boulevard
Golden, Colorado 80401-3393

13. Type of Report & Period Covered
Technical Report

14.

15. Supplementary Notes

SERI Contact: J. M. Parsons

16. Abstract (Limit: 200 words)

This report summarizes the results of preliminary studies conducted to identify and evaluate three innovative concepts for an open-cycle ocean thermal energy conversion (OTEC) steam turbine that could significantly reduce the cost of OTEC electrical power plants. The three concepts are (1) a crossflow turbine, (2) a vertical-axis, axial-flow turbine, and (3) a double-flow, radial-inflow turbine with mixed-flow blading. In all cases, the innovation invloves the use of lightweight, composite plastic blading and a physical geometry that facilitates efficient fluid flow to and from the other major system components and reduces the structural requirements for both the turbine or the system vacuum enclosure, or both. The performance, mechanical design, and cost of each of the concepts are developed to varying degrees but in sufficient detail to show that the potential exists for cost reductions to the goals established in the U.S. Department of Energy's planning documents. Specifically, results showed that an axial turbine operating with 33% higher steam throughput and 7% lower efficiency than the most efficient configuration provides the most cost-effective open-cycle OTEC system. The vacuum enclosure can be significantly modified to reduce costs by establishing better interfaces with the system.

17. Document Analysis

a. Descriptors

Solar power plants ; ocean thermal power plants ; ocean thermal energy conversion ; energy conversion

b. Identifiers/Open-Ended Terms

c. UC Categories

262

18. Availability Statement

National Technical Information Service
U.S. Department of Commerce
5285 Port Royal Road
Springfield, Virginia 22161

19. No. of Pages
71

20. Price
A04

Form No. 0069 (6-30-87)

*U.S. GOVERNMENT PRINTING OFFICE: 1990-0-773-107/00034